

COMPARTMENTALIZED RHO GTPASE ACTIVATION IS ASSOCIATED WITH
EFFECTS ON ACTIN BINDING PROTEINS

A DISSERTATION

SUBMITTED IN PARTIAL FULFILLMENT OF THE REQUIREMENTS FOR THE
DEGREE OF DOCTOR OF PHILOSOPHY
IN THE GRADUATE SCHOOL OF THE
TEXAS WOMAN'S UNIVERSITY

COLLEGE OF ARTS AND SCIENCES

BY

JENNIFER SEIFERT, B.S.

DENTON, TEXAS

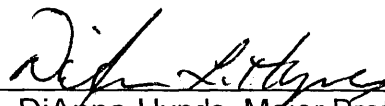
MAY 2008

TEXAS WOMAN'S UNIVERSITY
DENTON, TEXAS

April 4, 2008

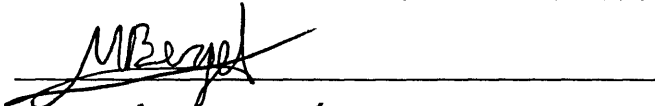
To the Dean of the Graduate School:

I am submitting herewith a dissertation written by Jennifer Seifert entitled "Compartmentalized Rho GTPase Activation is Associated with Effects on Actin Binding Proteins." I have examined this dissertation for form and content and recommend that it be accepted in partial fulfillment of the requirements for the degree of Doctor of Philosophy with a major in Molecular Biology.



DiAnna Hynds, Major Professor

We have read this dissertation and recommend its acceptance:



Lynnda Uphouse

Jammon Fuchs

Beulah No

Sarah A. McIntire

Department Chair

Accepted:



Dean of the Graduate School

ABSTRACT

JENNIFER SEIFERT

COMPARTMENTALIZED RHO GTPASE ACTIVATION IS ASSOCIATED WITH EFFECTS ON ACTIN BINDING PROTEINS

MAY 2008

Axon growth and guidance during development and regeneration is mediated by cytoskeletal dynamics in the neuronal growth cone, a structure at the leading edge of extending axons. Axon extension and retraction is regulated by the activity of members of the Rho family of small guanine nucleotide triphosphatases (GTPases), which include Rac1, RhoA and Cdc42. In neurons, Rac1 specifically promotes axon extension and RhoA inhibits growth cone extension. In non-neuronal cells, however, activation of Rho GTPases promotes the formation of complexes of actin binding proteins, promoting lamellipodial expansion (via Rac1), microspike formation (via Cdc42) and the formation of stress fibers (via RhoA). The unique cytoarchitecture of neurons may contribute to the different responses of neurons and other migratory cells, potentially via localized control over activation of specific Rho GTPases. If so, then differential Rho GTPase activity may lead to specific effects on the formation of complexes

of actin binding proteins in growth cones. Thus, we first assessed whether activation of RhoA and Rac1 was compartmentalized to specific cellular regions and then determined the effects of this activation on the co-localization and complexing of polymerization-promoting actin binding proteins. We found Rac1 was preferentially activated in the growth cones while RhoA activation was induced in both the somata and growth cones of B35 rat neuroblastoma cells. Treatments which promote Rho GTPase activation and outgrowth increased the co-localization of the actin binding proteins VASP, Arp3, WAVE and profilin. We also found that VASP forms a complex with Arp3 and profilin while WAVE only binds to Arp3, thus suggesting a difference in the molecular components of actin binding complexes between neuronal cells and those reported in non-neuronal cells. We interpret these results to indicate that signaling through the Rho GTPases can regulate the co-localization of proteins which promote the actin nucleation and polymerization necessary for axonal growth and guidance.

TABLE OF CONTENTS

	Page
ABSTRACT	iii
LIST OF TABLES	vii
LIST OF FIGURES	viii
Chapter	
I. INTRODUCTION.....	1
Growth Cone Actin Dynamics in Axon Growth and Guidance	3
Rho GTPases in Axon Growth and Guidance	4
Extracellular Cues That Promote Outgrowth	5
Extracellular Cues That Inhibit Outgrowth	7
Rho GTPase Signal Transduction	9
Activation of Rho GTPases	9
Downstream Effects of Rho GTPases	12
RhoA and Rac1 Effectors	12
ROCK, PAK, and Formins	12
Actin Binding Proteins	16
Summary	20
II. METHODS	23
Cell Culture and Treatment	23
Measurement of Rho GTPase Activation	25
Treatment Groups	25
Growth Cone Fractionation.....	25
Analysis of Growth Cone Fractionation Technique.....	26
Pull-Down Assay	27
Western Blotting	28
Measurement of RhoA Activation by ELISA	28

Localization of Actin Binding Proteins in Growth Cones.....	30
Treatment Groups	30
Immunocytochemistry	30
Measurement of Complex Formation of Actin-Binding Proteins	32
Treatment Groups	32
Co-immunoprecipitation	33
III. RESULTS.....	35
Rac1 Activation Levels are Induced Within the Growth Cone	38
RhoA Activation Levels are Induced Within the Cell Body and Growth Cones	42
Actin Binding Proteins Localize to the Growth Cone When Treated with Rho GTPase Signaling Modulators.....	45
Co-localization of Actin Binding Proteins Within the Growth Cone Increases When Treated With Rho GTPase Modulators	55
Arp3 Binds to WAVE and VASP, but Profilin Only Binds to VASP	65
IV. DISCUSSION	73
Activation of Rho GTPases by Outgrowth Promoters and Inhibitors	74
Compartmentalization of the Rho GTPase Activation	75
Localization of Actin Binding Proteins Increases in the Growth Cone in Response to Outgrowth Promoting Treatments.....	76
Co-Localization of Actin Binding Proteins Increases in the Growth Cone in Response to Outgrowth Promoting Treatments.....	77
Molecular Components of Actin Binding Complexes are Different Than Non-neuronal Cells	79
Rho GTPase Activation and Actin Binding Proteins	80
Summary.....	83
REFERENCES.....	84
APPENDIX.....	97

LIST OF TABLES

	Page
Table	
1: Summary of the effects of each treatment on neurite outgrowth and Rho GTPase activation.....	24

LIST OF FIGURES

Figure	Page
1 Diagram of a neuronal growth cone	2
2 Summary of actin dynamics	17
3 Proposed signaling pathways for the regulation of actin dynamics by Rho GTPases in growth cones.....	22
4 Cell fractionation yields a fraction enriched for growth cones	37
5 Rac1 activation in whole cell lysates and growth cone fractions	40
6 RhoA activation in B35 whole cell lysates and growth cone fractions.....	44
7 Co-localization of actin binding proteins in growth cones.....	46
8 Arp3 localization in B35 growth cone regions.....	49
9 VASP localization in B35 growth cone regions.....	50
10 WAVE localization in B35 growth cone regions.....	52
11 Profilin localization in B35 growth cone regions	53
12 Co-localization of WAVE and VASP.....	56
13 Co-localization of VASP and profilin.....	58
14 Co-localization of WAVE and profilin.....	59
15 Co-localization of WAVE and Arp3.....	60
16 Co-localization of Arp3 and profilin.....	63

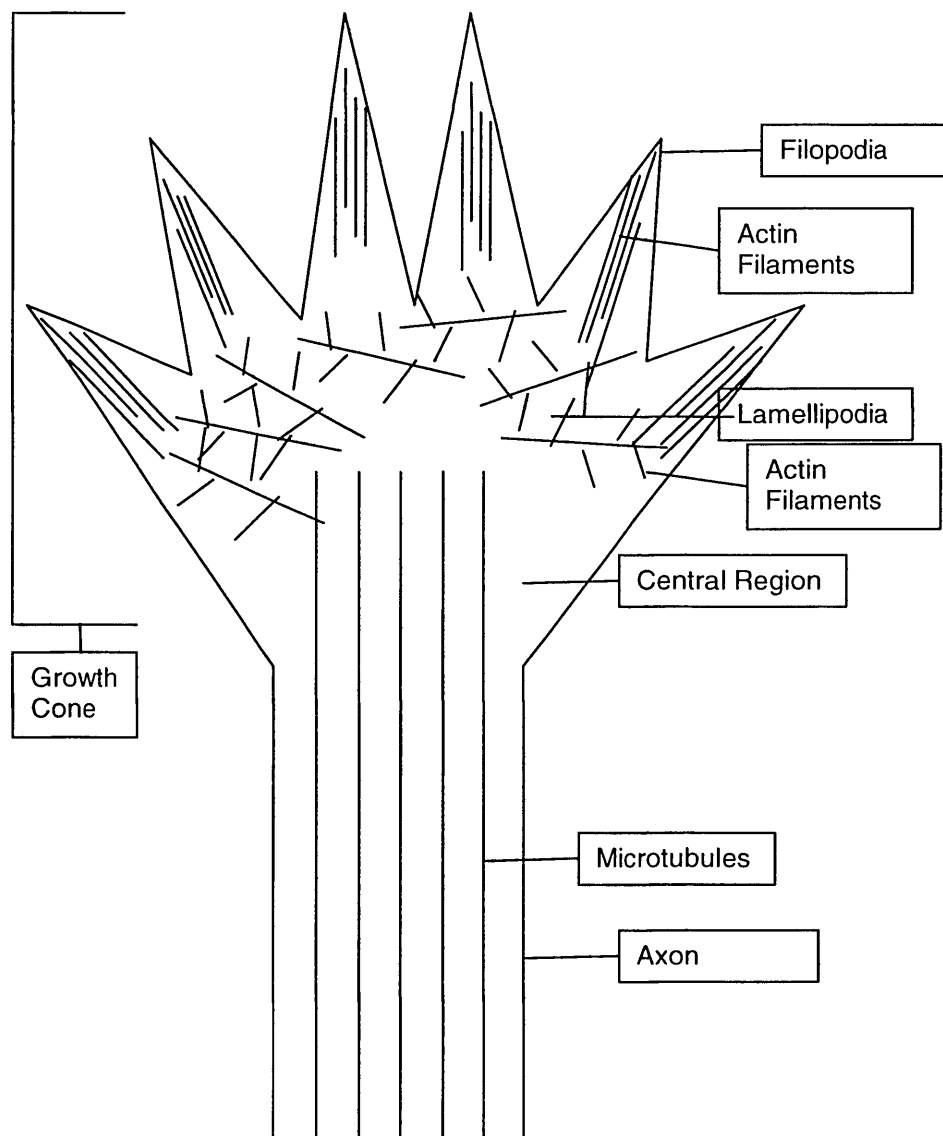
17	Co-localization of Arp3 and VASP	64
18	Negative control blot to ensure limited interference from the heavy chain of the precipitating antibody	67
19	WAVE binds to Arp3.....	68
20	WAVE does not bind to profilin.....	70
21	VASP binds to Arp3.....	71
22	VASP binds to profilin.....	72
23	Proposed model for Rho GTPase activation and their associated effects on actin binding proteins	82

CHAPTER I

INTRODUCTION

Spinal cord injuries result in a disruption of neuronal axon extension that precludes the correct reinnervation of target cells located across the scar site. Understanding the molecular mechanisms that regulate axonal growth and guidance may aid our ability to manipulate intracellular signaling to promote recovery following injury or degeneration. Neuronal growth cones, located at the leading edge of extending axons, respond to extracellular cues to mediate axon extension and pathfinding during development or regeneration. Growth cones contain dynamic actin-based structures which are rearranged in response to extracellular cues. These structures consist of filopodia in which actin filaments are arranged in longitudinal bundles, and lamellipodia which contain a meshwork of actin filaments (Schaefer et al., 2002) (Fig. 1). Soluble actin monomers (G actin) are preferentially added onto the barbed (plus) ends of filamentous actin (F actin) and removed from the pointed (minus) ends (depolymerization) in vivo. Growth cone and actin filament dynamics are regulated in part by the Rho subfamily of guanine nucleotide triphosphatases (GTPases), including RhoA and Rac1 (Rashid et al., 2001; Nusser et al., 2005). These small G proteins direct actin rearrangements via activation of downstream effectors. Understanding Rho

Figure 1: Diagram of a neuronal growth cone. Growth cones are composed of lamellipodial, filopodial and central regions, which are supported by a meshwork of actin filaments, longitudinally bundled actin filaments, and microtubules, respectively.



GTPase activation and subsequent effects on neurite outgrowth may lead to therapeutic strategies to enhance recovery following nervous system damage.

Growth Cone Actin Dynamics in Axon Growth and Guidance

The processes necessary for axon growth and guidance involve the lamellipodial, filopodial, and central regions of the neuronal growth cone (Fig. 1). Actin dynamics within the lamellipodia are believed to drive growth cone advance, while filopodia are essential for sensing stimulatory and inhibitory extracellular cues (Meyer and Feldman, 2002; Matsuura et al., 2004). Axon growth has three identified phases consisting of protrusion, engorgement, and consolidation (Rosdahl et al., 2003). Protrusion is the process of lamellipodial and filopodial extension from the growth cone while engorgement refers to the influx of organelles and microtubules into the newly expanded areas. Consolidation is the formation of new axon behind the growth cone and requires an inhibition of protrusion; this allows for the maintenance of cell polarity. All three processes are necessary for outgrowth to occur and thus require a coordination of multiple signaling pathways. In addition to the polymerization of G actin into F actin, nucleation (branching) of F-actin and capping of F-actin at the

barbed end (Schmidt et al., 1995; Meyer and Feldman, 2002) are important mechanisms utilized to bring about changes to the actin cytoskeleton. These changes are essential for the promotion of axon growth and guidance. Thus, in an extending growth cone, actin must polymerize at the leading tips of filopodia while nucleation occurs in the lamellipodia. To support these changes in actin structures at the leading edges of growth cones, microtubules in the central region are also undergoing rearrangement (Gallo and Letourneau, 2004).

Rho GTPases in Axon Growth and Guidance

Studies in non-neuronal cell types have shown that RhoA regulates the formation of stress fibers, Rac1 regulates the formation of membrane ruffles in the lamellipodia and Cdc42 regulates microspike initiation leading to filopodial formation (Kozma et al., 1997; Ridley et al., 1999). In neurons, the Rho GTPases regulate neurite extension, retraction, and turning. Specifically, RhoA is associated with neurite retraction or growth cone collapse while Rac1 and Cdc42 promote neurite extension (Kozma et al., 1997; Vastrik et al., 1999; Wahl et al., 2000).

During development, Rho GTPases are necessary to establish functional neuronal patterns. Specifically, they have been linked to neuronal migration,

axon formation and outgrowth, and dendritic spine formation and maintenance (Govek et al., 2005). Mutations in the regulators or effectors of Rho GTPase signaling lead to neurological disorders such as mental retardation and amyotrophic lateral sclerosis (ALS), reflecting their importance in development (Newey et al., 2005).

Following spinal cord injury, neurons are exposed to factors in the blood, such as lysophosphatidic acid (LPA), that produce inhibitory effects. LPA is a G-protein coupled receptor (GPCR) agonist that acts through the $G\alpha_{12-13}$ subunits (Moolenaar et al., 1997; Gutkind, 1998). Treatment with LPA or $G\alpha_{12-13}$ leads to RhoA activation, neurite retraction and growth cone collapse (Kranenburg et al., 1999). In order to understand how to overcome the inhibitory effects of the scar site to axon outgrowth, we must understand the effects of axon guidance molecules on growth cone dynamics and Rho GTPase activation and subsequent signaling pathways.

Extracellular Cues That Promote Outgrowth

Axon guidance factors are categorized by their solubility and effect on neurite outgrowth. For example, chemoattractants are freely diffusible molecules that promote outgrowth and contact attractants are those that are bound to the extracellular matrix or surface of cells (Bonner and O'Connor, 2001). Netrin is a chemoattractant which induces growth cone turning via activation of Rac1 and

Cdc42. Netrin signaling is transduced by receptor tyrosine kinases (RTK). This signaling increases intracellular calcium levels in addition to the activation of Rac1 and Cdc42 (Liu et al., 1998). Neurotrophins, such as nerve growth factor (NGF) and brain-derived neurotrophic factor (BDNF) also signal through RTK receptors to induce growth cone turning (Gallo and Letourneau, 2004). Laminin is a contact attractant that also activates these GTPases to guide growth cone advance. Laminin signals through integrin receptors which may indirectly increase intracellular cAMP (Bonner and O'Connor, 2001).

Calcium regulates Rho GTPase activity in a protein kinase C (PKC) dependent manner within the growth cones of *Xenopus* spinal neurons (Jin et al., 2005). This study by Jin and colleagues (2005) sought to definitively determine the relationship between calcium and Rho GTPases and their role in growth cone navigation, based on previous studies showing that calcium regulated Rho GTPases (del Pozo et al., 2000) and, conversely, Rho GTPases can regulate calcium dynamics (Singleton and Bourguignon, 2002). Specifically, Jin and colleagues (2005) found that direct elevation of calcium (by ryanodine treatment) can activate Rac1 and Cdc42, but inactivate RhoA, and that this downstream activation of the GTPases by calcium is carried out via PKC and induces growth cone turning. Cross-talk patterns between cAMP and calcium have been established showing that intracellular calcium can affect cAMP levels by modulating either phosphodiesterase or adenylyl cyclase activity (Beavo and

Reifsnnyder, 1990; Choi et al., 1993). Conversely, cAMP signaling can also affect calcium levels by regulating calcium ion channel activity (Hell et al., 1994; Nishiyama et al., 2003).

An increase in intracellular cAMP levels in cortical neurons has been associated with dephosphorylation of ADF/cofilin. This modification results in an increase in neurite outgrowth (Meberg et al., 1998). cAMP has also been shown to promote differentiation and outgrowth in neuroblastoma cells (Otey et al., 2003). Because these chemo- and contact attractants mediate their effects via cAMP (Jin et al., 2005) and cAMP has been shown to effectively promote outgrowth in our model system (Hynds et al., submitted), we use a cAMP analog in these studies to promote outgrowth.

Extracellular Cues That Inhibit Outgrowth

In analogy to outgrowth promoters discussed above, chemorepellents and contact repellents inhibit neurite outgrowth. Among other inhibitory molecules, the scar produces chondroitin sulfate proteoglycans (CSPGs) which inhibit neurite growth (Spencer et al., 2003). It has been shown that activation of Rac1 and Cdc42 as well as inactivation of RhoA or its downstream effector, Rho kinase (ROCK), can overcome the CSPG-dependent inhibition of neurite extension (Jain et al., 2004).

Another set of proteins, found in the scar site, Nogo-A and myelin-associated glycoprotein (MAG), alter the ratio of active to inactive Rho GTPases. In particular, Nogo-A and MAG activate RhoA while at the same time inactivate Rac1. These proteins are inhibitory to neurite outgrowth, but this effect can be abolished by the inactivation of RhoA or Rho kinase with C3 transferase or Y27632, respectively (Niederost et al., 2002).

Semaphorins are an important family of guidance molecules which induce mainly repulsive activities in several types of neurons (Raper, 2000). Semaphorin effects are mediated by plexins (a class of receptors), either by binding directly or forming a complex to facilitate ligand binding, as is the case with class 3 semaphorins (Tamagnone et al., 1999; Tamagnone and Comoglio, 2000). In a study done in 2002, semaphorin 4D was found to bind to and activate plexin-B which then regulates PDZ-RhoGEF and LARG, two Rho guanine nucleotide exchange factors (RhoGEFs) (Swiercz et al., 2002). This regulation of the RhoGEFs led to RhoA activation. In a follow-up study done in 2004, the same group found that the plexin-B family of receptors are stably associated with the receptor tyrosine kinase, ErbB-2. Upon binding of semaphorin 4D to plexin-B1, ErbB-2 is stimulated to phosphorylate both plexin-B1 and itself. The phosphorylation of plexin-B1 is crucial for the activation of RhoA and its downstream effects (Swiercz et al., 2004). Another soluble semaphorin, collapsin-1 (also known as semaphorin 3A), also mediates growth

cone collapse but signals through both Rac1 (Kuhn et al., 1999) and RhoA (Hall et al., 2001).

The studies discussed above indicate the importance of the balance of activation amongst different Rho GTPases in determining the growth outcome of the cell in response to inhibitory molecules that are often upregulated after injury. In the experiments described herein, we use a soluble form of CSPGs and semaphorin 3A (sema 3A) to inhibit neurite outgrowth and assess Rho GTPase activation.

Rho GTPase Signal Transduction

Activation of Rho GTPases

The Rho family of small G proteins cycle between an active (GTP bound) state and an inactive (GDP bound) state. GTPases are regulated by guanine nucleotide exchange factors (GEFs) which exchange a GDP molecule for a GTP molecule. They are also regulated by GTPase activating proteins (GAPs), which induce the intrinsic ability of GTPases to hydrolyze GTP thus inactivating the protein, and guanine nucleotide dissociation inhibitors (GDIs) which prevent the exchange of GDP for GTP (Etienne-Manneville and Hall, 2002). There are many different GAPs, GEFs and GDIs, some of which are specific to a particular Rho GTPase, and some which can regulate more than one GTPase.

Traditionally, the activation and downstream effects of RhoA, Rac1, and Cdc42 was thought to act in separate and parallel pathways with their activation leading to neurite retraction/collapse, lamellipodial expansion, or filopodial elongation respectively (Kozma et al., 1997; Ridley et al., 1999). However, it is more likely that these three Rho GTPases affect the activation states of one another in addition to exerting their downstream effects. One group has studied the cross-talk between the Rho GTPases using a computational approach derived from Michaelis-Menton kinetics, along with empirical observations, and found that Rho GTPases can activate one another according to the following model (Sakumura et al., 2005). Cdc42 activates Rac1 and inhibits RhoA; Rac1 activates RhoA; and RhoA inhibits both Rac1 and Cdc42. Varying extracellular cues result in activation of different effectors of the Rho GTPases. Some of the signaling specificity of these regulators may be due to their association with scaffolding proteins that link them to the GTPase and a particular effector protein (Buchsbaum et al., 2002; Jaffe et al., 2004).

A new theory is emerging, however, that further complicates issues regarding Rho GTPase regulation of actin dynamics. According to this theory, not only is the balance of Rho GTPase activation important for predicting actin dynamics and growth cone behaviors, but the intracellular location of protein activation is just as pertinent. In a recent study, Nakamura and colleagues (2005) showed that all three GTPases were active in the peripheral domain of the

growth cone while RhoA was also active in the shaft and central domain. They saw that RhoA activation in the shaft of neuroblastoma cells resulted in neurite retraction, while RhoA activation in the peripheral domain was necessary to maintain the spread morphology of growth cones (Nakamura et al., 2005).

In a related study, Nakamura and colleagues assessed growth cone localization of Rho GTPase activation using fluorescence resonance energy transfer (FRET) analysis. CFP/YFP probes containing downstream effector binding sites for active Rho GTPases were utilized to observe the activation of Rac1 and Cdc42 localized to the neurite tips of PC12 cells upon stimulation with NGF (Nakamura et al., 2005). The authors observed that upon stimulation with NGF, phosphatidylinositol 3,4,5-trisphosphate (PIP₃) accumulated, leading to the recruitment of Vav2 and Vav3 which are known GEFs (Altun-Gultekin et al., 1998). Vav2/3 activated Rac1 and Cdc42, leading to neurite outgrowth as well as the activation of PI3-kinase. It is possible that activation of Rho GTPases is spatially regulated.

Both of these studies assessed the localization of Rho GTPase activation using FRET. They raised the intriguing possibility of localization of GTPase activity. However, FRET results are often difficult to interpret and are dependent on the molecular characteristics of the probe. Thus, we assessed Rho GTPase activation localized to growth cones using biochemical methods including growth cone fractionation and western blot analysis.

Downstream Effects of Rho GTPases

RhoA and Rac1 Effectors

Previous studies have shown that RhoA regulates the formation of stress fibers, Rac1 regulates the lamellipodia (membrane ruffles) while Cdc42 regulates the filopodia (microspikes) (Ridley and Hall, 1992; Ridley et al., 1992; Kozma et al., 1997). The question remains, once these Rho GTPases are activated, how do they regulate the actin cytoskeleton dynamics within the neuronal growth cone? Many studies in non-neuronal cells have shown a link between downstream effectors of the Rho GTPases and actin binding proteins that work in complexes to promote changes to the actin cytoskeleton. Immediate downstream effectors for Rho GTPases include serine threonine kinases that activate actin binding proteins.

ROCK, PAK, and Formins

The immediate downstream effectors for active Rho GTPases are well established. GTP-bound RhoA activates Rho-associated, coiled-coil-forming protein kinase (ROCK), Cdc42 activates the Wiskott-Aldrich Syndrome protein (WASP) and both Rac1 and Cdc42 activate p21-activated kinase (PAK) (Bishop and Hall, 2000). Though these effectors carry out a multitude of functions, it is our intent to focus on their effects on the actin cytoskeleton in this study.

In neurons, ROCK is believed to be responsible for the process of consolidation. In a study by Loudon and colleagues (2006), the authors found that ROCK inhibits F-actin polymerization at the leading edge (protrusion) while enhancing the myosin II-dependent contractility at the neck region of the growth cone. This study also showed that the ROCK and myosin II driven process of consolidation was an important part of axon guidance.

ROCK also plays a role in the stabilization of point contacts following their formation in a Rac1-dependent manner (Costigan et al., 1998). Previous studies had shown that adhesion to the extracellular matrix (ECM) was essential for growth cone motility and axon guidance (Ridley et al., 2003; Suter et al., 2004) and that this process involved both Rac1 and RhoA in fibroblasts (Mackay et al., 1995). In a more recent study, Woo and Gomez (2006) found that in growth cones, the initial formation of point contacts was achieved through Rac1 activation at the leading edge, while stabilization of these contacts required Rac1 inactivation and activation of ROCK (through RhoA signaling). This coordination of activation led to rapid neurite outgrowth through the formation of point contacts and the stabilization of membrane ruffles.

The ECM has been shown to have an effect on signaling through Rac1, specifically by PAK activation (del Pozo et al., 2000). The authors found that growth factors and attachment to the ECM contributed equally to the activation of Rac1, but that adherent cells were able to activate PAK while floating cells were

not. When Rac1 is bound to GTP, it is able to bind PAK which is then autophosphorylated to activate its serine/threonine kinase activity (Knaus and Bokoch, 1998). Activated Rac1 translocated to the membrane in adherent cells but remained in the cytoplasm of suspended cells. A mutated form of Rac1 that was unable to translocate to the membrane was unable to activate PAK, while conversely, a form of Rac1 which is forced to interact with the membrane in suspended cells was now able to activate PAK (del Pozo et al., 2000). The authors showed that adhesion to the ECM regulated anchoring sites for Rac1 to associate with the membrane. These data indicate that membrane translocation of active Rac1 may be critical for its downstream effects: activation of PAK. A model for this effect was proposed by Marc Symons in which cytosolic GDP-bound Rac1 is complexed with GDI and upon activation dissociates from GDI and (in adherent cells) is translocated to the membrane (Symons, 2000). This membrane-tethered, active Rac1 can then bind to and activate PAK.

Another player was introduced which recruits PAK to the membrane, further validating the above model. Several early studies showed that Nck, an SH2-SH3 adapter protein, recruits PAK to the membrane by tethering it to receptor tyrosine kinases for epidermal growth factor (EGF) and platelet-derived growth factor (PDGF) (Li et al., 1992; Nishimura et al., 1993; Benard et al., 1999). Nck was shown to interact with PAK through its second SH3 domain.

This association leads to the phosphorylation of Nck and provides a link between PAK and cell activating growth hormones (Benard et al., 1999).

Earlier we discussed the activation of RhoA by Sema4D signaling through the plexin-B receptor. It appears that this signaling also modulates Rac1 activity (Vikis et al., 2002). Interaction between active Rac1 and plexin-B1 can inhibit PAK activation and, interestingly, activation of Rac1 enhances the binding of semaphorin 4D to plexin-B1. This bi-directional interaction leads to a model where Rac1 modulates plexin-B1 activity and plexin-B1 modulates Rac1 activity.

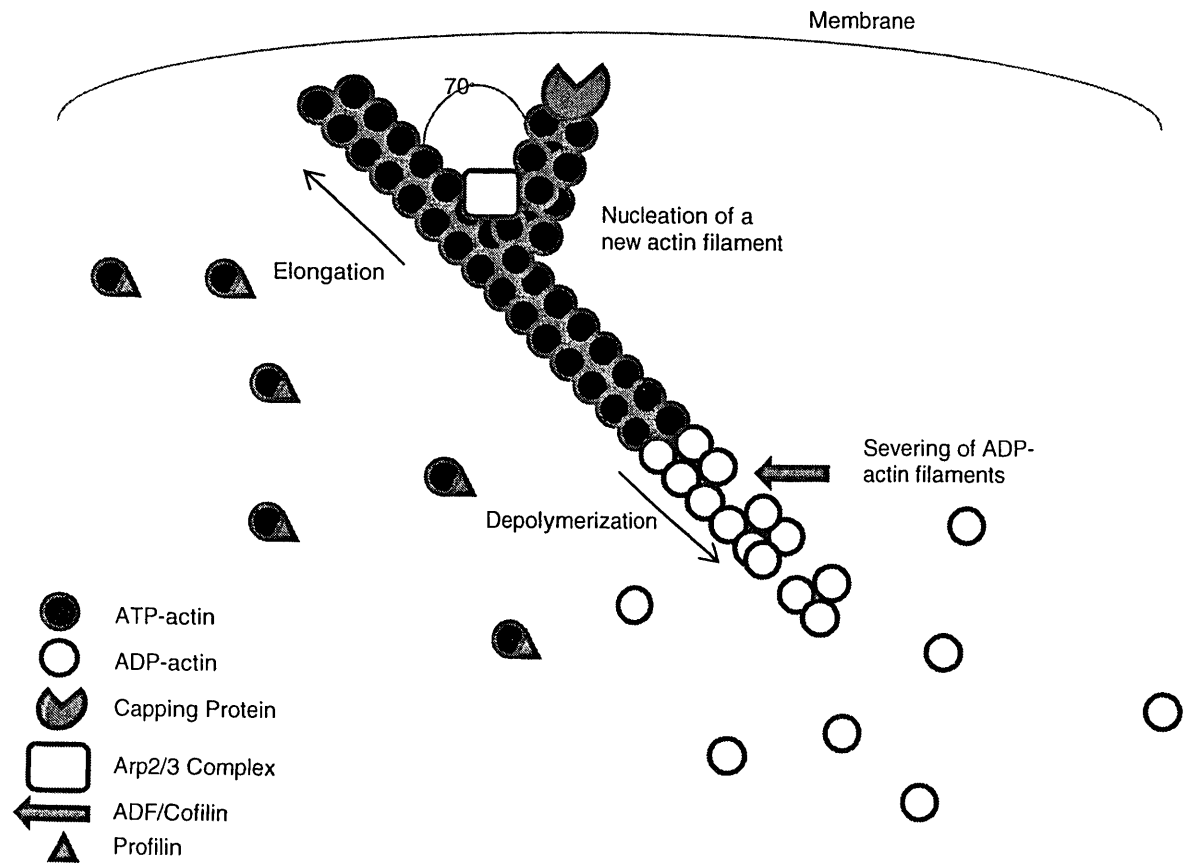
Whether PAK regulates actin dynamics in navigating growth cones is still somewhat controversial. However, PAK may activate another Rho GTPase effector, LIM-kinase, that is a potential regulator of actin dynamics. LIM-kinase catalyzes the phosphorylation of cofilin, an actin binding protein, thereby inactivating its actin-depolymerizing activity (Tigyi et al., 1996). Previous studies have shown that LIM-kinase acts downstream of Rac1, but is not a direct substrate (Tigyi et al., 1996; Arber et al., 1998). Authors of a recent study found that PAK1, upon activation by either Rac1 or Cdc42, transphosphorylates and activates LIM kinase (Edwards et al., 1999). This leads to phosphorylation and inactivation of cofilin and thus decreased depolymerization of F-actin. In a related study, the authors found that LIM kinase can be activated by ROCK in addition to PAK1 by phosphorylation at threonine 508 of the activation loop (Bito et al., 2000).

Another class of proteins, the formins, are also direct effectors of active Rho GTPases (Watanabe et al., 1999; Alberts, 2001). This group of proteins serves to nucleate actin filaments, though they do not bind directly to actin (Pruyne et al., 2002; Sagot et al., 2002). mDia2, which is one type of formin, was also found to bundle actin filaments and promote processive capping in addition to its nucleation function (Harris et al., 2006; Moseley et al., 2006). The above discussed effector proteins of RhoA and Rac1 modulate actin binding proteins in order to exert changes in the actin cytoskeleton.

Actin Binding Proteins

Actin dynamics encompass a range of mechanisms which work cooperatively to promote or inhibit axon growth and guidance. These mechanisms are regulated by complexes of actin binding proteins. There are many actin binding proteins which regulate not only depolymerization, but also polymerization of G actin into F actin, nucleation (branching) of F-actin, as well as capping of F-actin at the barbed end (Schmidt et al., 1995; Meyer and Feldman, 2002). These changes to the actin cytoskeleton are depicted in Figure 2. In particular, a complex of WAVE and the Arp2/3 complex promotes actin branching and a complex of WASP and Arp2/3 promotes longitudinal polymerization.

Figure 2: Summary of actin dynamics including polymerization, depolymerization, capping, nucleation, and severing.



WAVE (Scar), a WASP-family protein, induces actin reorganization downstream of Rac1, thereby promoting the formation of membrane ruffles through activation of Arp2/3 (Abe et al., 2003). The Arp2/3 complex, with help from WAVE, is responsible for nucleation of new filaments (Mullins et al., 1998). Phosphatidylinositol 4-phosphate 5-kinase has also been shown to play a role in the formation of membrane ruffles via direct interaction with active Rac1 which leads to the production of phosphatidylinositol 4,5-bisphosphate (PIP₂) through the phosphorylation of PIP. PIP₂ can then either be cleaved to produce the second messengers inositol trisphosphate (IP3) and diacylglycerol (DAG) or can bind directly to actin binding proteins such as profilin, cofilin, gelsolin, and α -actinin, regulating their functions (Stossel, 1993).

This above mentioned process of membrane ruffling appears to mirror the Cdc42 driven association of the Arp2/3 complex with WASP to promote filopodial formation and extension. The Arp2/3 complex, with help from WASP and neuronal WASP (N-WASP), is responsible for the promotion of actin polymerization (Mullins et al., 1998). This would indicate that the role of Arp2/3 is dependent upon the proteins with which it is complexed.

Various groups have looked at how ROCK may exert changes in actin dynamics. One group showed that activation of RhoA and ROCK led to neuritogenic arrest, and conversely, their inhibition resulted in accelerated neuritogenesis (Da Silva et al., 2003). The authors of this study also found that

profilin IIa (P11a), an actin binding protein found mainly in the brain (Witke et al., 2001), forms a complex with ROCK and this complex is regulated by RhoA activity. Da Silva and colleagues (2003) hypothesize that when RhoA is in its active, GTP-bound state, ROCK complexes with P11a and phosphorylates it, forming a neuritogenic-arrest complex. Upon proper extracellular stimuli, RhoA becomes inactivated, causing ROCK to dissociate from P11a, resulting in lower levels of phosphorylated P11a. This results in changes to the filamentous/soluble actin ratio, leading to neurite initiation. Profilin and capping proteins, also actin binding proteins, can also act in conjunction with the Arp2/3 complex to promote or inhibit polymerization, respectively (Blanchoin et al., 2000).

Ena and VASP proteins appear to compete with capping proteins to allow the polymerization of soluble actin into longer F-actin (Bear et al., 2000). In VASP deficient cells, the cell volume is unchanged though the cell covers twice as much area as compared to wildtype cells (Garcia Arguinzonis et al., 2002). Also in these mutant cells, activation of the Rac1/ PAK signaling pathway is greatly increased and prolonged following treatment with PDGF or serum.

These studies demonstrate that Rho GTPase signaling can control the formation of complexes of actin binding proteins in non-neuronal cells. However, whether these same mechanisms work in neurons remains to be determined. In the experiments reported here, we determine how manipulation of Rho GTPase activation affects association of actin binding proteins.

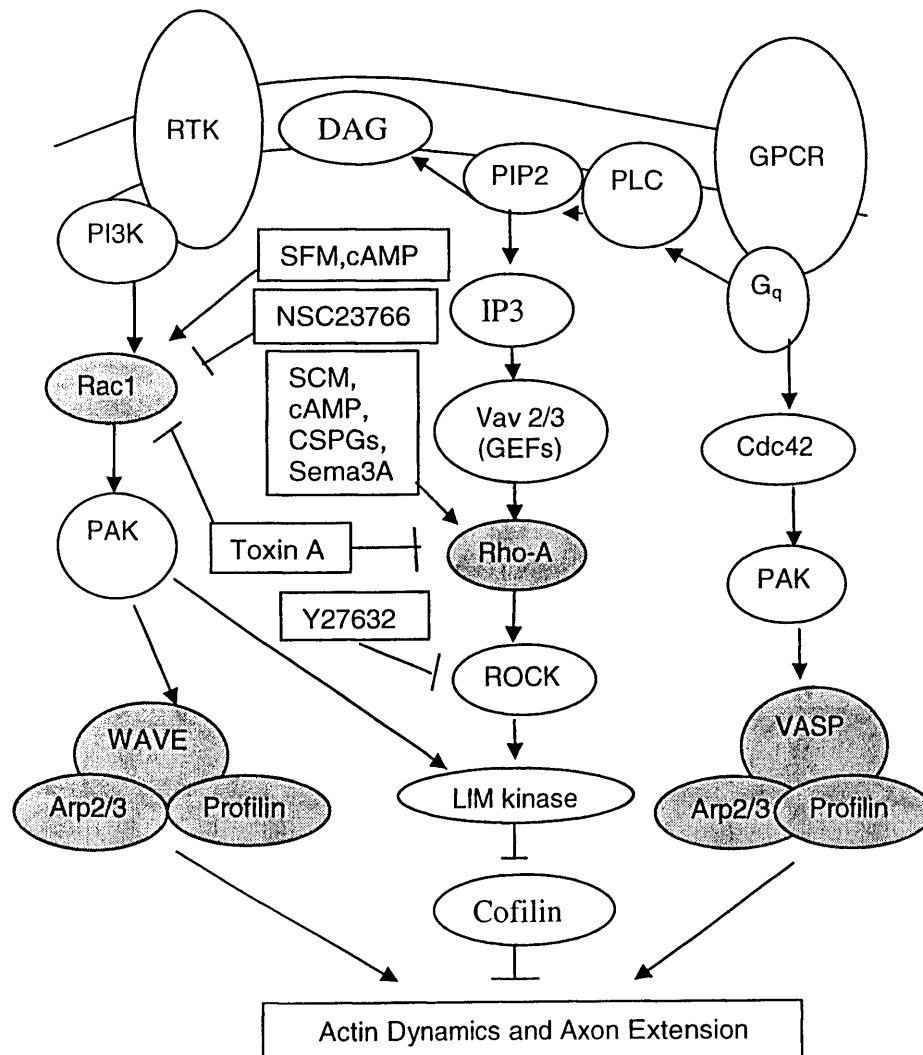
Summary

In recent studies, much advancement has been made towards the elucidation of the signal transduction pathways that result in actin remodeling and axon growth and guidance. Connections have been found between the Rho GTPases and proteins that control actin dynamics as well as links between the opposing functions of RhoA and Rac1/Cdc42. As more proteins are found to be involved with the remodeling of the actin cytoskeleton and further interactions between pathways are revealed, the model for how the growth cone is remodeled in response to extracellular signals will continue to grow in complexity. Based on these previous studies, we propose that Rac1 promotes axon extension through the formation of complexes that promote actin nucleation (WAVE, Arp2/3 and profilin) and polymerization (VASP, Arp2/3 and profilin). Much of the work described above was performed using non-neuronal migratory cells. However there are significant differences in the cytoarchitecture of growth cones as compared to migratory cells. Thus it is possible that regulation of actin dynamics differs significantly in these cell populations.

We hypothesize that outgrowth promoting treatments will activate Rac1 in the growth cone while inhibitory treatments will increase RhoA activation in the growth cone. Furthermore, we believe that treatments which activate Rac1 will produce co-localization and complex formation of actin binding proteins within the

lamellipodial region of the growth cone. Conversely, inhibitory treatments will promote lower levels of actin binding complexes. We have tested the localization of RhoA and Rac1 activation as well as the co-localization and complexing of WAVE, Arp3, VASP and profilin. Figure 3 shows our proposed model of Rho GTPase signaling pathways and how they relate to actin dynamics, as well as the specific components tested in this study.

Figure 3: Proposed signaling pathways for the regulation of actin dynamics by Rho GTPases in growth cones. Extracellular cues activate membrane-bound receptors to initiate signaling cascades leading to Rho GTPase activation. This activation promotes formation of molecular complexes that regulate actin dynamics. Shaded components indicate aspects of the proposed model which we tested, and treatments with their reported or proposed effects are indicated in rectangles.



CHAPTER II

METHODS

Cell Culture and Treatment

B35 rat neuroblastoma cells (ATCC, Manassas, VA) were routinely maintained at 37°C in 1:1 Dulbecco's Modified Eagle's Medium and Nutrient Mixture F12 (DMEM/F12; Invitrogen, Carlsbad, CA) supplemented with 10% fetal bovine serum (FBS; Sigma, St. Louis, MO) and passaged when 90% confluent. The cells for experiments were seeded in 10 cm plates at 20,000 cells/cm² for measurement of RhoA and Rac1 activation and on 12 mm glass coverslips at a density of 5,000 cells/cm² for immunocytochemistry experiments. Cells were allowed to grow to the appropriate density (see individual experimental methods below) and were either maintained in serum-containing medium (SCM) or were washed with phosphate buffered saline (PBS) and placed into serum free media (SFM) for 24 hours. In all experiments, maintenance in SCM provided a baseline and cells were treated to promote or inhibit neurite outgrowth. Outgrowth-promoting treatments included SFM and 10 μM 8-bromoadenosine-5',3'-cyclic monophosphate (8-Br-cAMP, Sigma, St. Louis, MO); outgrowth-inhibiting treatments included 5 μg/ml chondroitin sulfate proteoglycans (CSPGs;

Chemicon, Temecula, CA) or 50 ng/mL semaphorin 3A (sema3A; R & D Systems, Minneapolis, MN). In some experiments, inhibitors of Rho GTPase signaling, including the general Rho GTPase inhibitor *Clostridium difficile* Toxin A (10 ng/mL; EMD Biosciences, San Diego, CA), the Rho kinase inhibitor Y27632 (5 μ M; EMD Biosciences, San Diego, CA), and the Rac1 inhibitor NSC23766 (100 μ M; EMD Biosciences, San Diego, CA) were used. Table 1 summarizes the known or proposed effects of each treatment.

Table 1: Summary of the effects of each treatment on neurite outgrowth and Rho GTPase activation.

Treatment	Effect on Outgrowth	Effect on Rho GTPases
SCM	Inhibitory (2)	Activates RhoA (1)
SFM	Stimulatory (2)	Activates Rac1 (1)
8-Br-cAMP	Stimulatory (2)	Activates Rac1, RhoA (1)
CSPGs	Inhibitory (7)	Activates RhoA (1)
Sema3A	Inhibitory/GC Collapse (6)	Activates RhoA (1)
Toxin A	Stimulatory (1)	Inhibits RhoA, Rac1 (3)
NSC23766	Stimulatory (1)	Inhibits Rac1 (4)
Y27632	Stimulatory (1)	Inhibits ROCK (5)

(1) Proposed effect, (2) Otey et al., 2003, (3) McCloskey and Zhang, 2000,

(4) Desire et al., 2005, (5) Watanabe et al., 2007, (6) Raper, 2000,

(7) Domeniconi, 2005.

Measurement of Rho GTPase Activation

Treatment Groups

Rac1 activation was measured by pull-down assays and activation of RhoA was measured using a commercially available enzyme-linked immunoabsorbance (ELISA) based kit. The pull-down assay utilized p21-activated kinase (PAK, will bind to active forms of Rac1) bound to agarose beads in order to discriminate between active and inactive forms of Rac1. In both sets of experiments, cells were grown to confluency in 10 cm plates and maintained in SCM or placed into SFM and either not treated or treated for 15 minutes with 10 μ M 8-Br-cAMP, 5 μ g/ml CSPGs, 50 ng/ml sema3A, 8-Br-cAMP plus CSPGs, or 8-Br-cAMP plus sema3A. Cells were either lysed directly in an IGEPAL CA-630 lysis buffer (1.0% IGEPAL CA-630, 1.5 mM EDTA, 25 mM Tris-HCl (pH=7.4), and 150 mM NaCl) or fractionated (see next section) and lysed.

Growth Cone Fractionation

To separate growth cones from cell bodies, we used differential centrifugation (Meyerson et al., 1992; Stettler et al., 1999). Following treatment, cells were homogenized in EDTA buffer (0.5 mM EDTA, 137 mM NaCl, 10 mM Na_2HPO_4 , 2.7 mM KCl, and 0.15 mM KH_2PO_4) using a Teflon/glass homogenizer and fractions were separated by differential centrifugation on a 20%

sucrose cushion at 500 x *g* for 4 minutes. Growth cones were collected at the sucrose cushion/EDTA buffer interface while the remainder of the cells pelleted at the bottom of the tube. A glass transfer pipet was used to extract each fraction which was placed in fresh microcentrifuge tubes. The excess sucrose solution was removed from each fraction by spinning the samples at 14,000 x *g* for 20 minutes and discarding the supernatant. Fractions were then lysed on ice in IGEPAL CA-630 buffer. Samples were either used immediately or stored at -20°C.

Analysis of Growth Cone Fractionation Technique

To determine the effectiveness of cell fractionation resulting in isolation of growth cones, we used a growth cone specific antibody to marker 2G13. We immunolabeled fixed B35 cells with anti 2G13 (1:1000 dilution; AbCam, Cambridge, MA) to show localization of this marker to growth cones. Standard immunocytochemical procedures were used, as described in the methods section for immunocytochemistry. Then, B35 cells, fractionated as previously described, were lysed and western blotted for 2G13 as described in the western blotting procedural section.

Pull-Down Assay

Pull-down assays were used to compare the ratio of active Rac1 to total Rac1 in order to analyze changes in activation levels of Rac1 in response to various treatments. Following analysis of protein content via a Pierce BCA protein assay, lysates (200-400 μ g total protein) were incubated for 45 minutes at 4°C with 20 μ g PAK protein binding domain (PAK-PBD)-conjugated agarose beads (Cytoskeleton, Denver, CO) to pull down active Rac1. PAK was used in excess to ensure that all active Rac1 would be bound as demonstrated previously (Benard et al., 1999). Beads were washed three times in wash buffer (25 mM Tris pH 7.5, 30 mM MgCl₂, and 40 mM NaCl) to remove nonspecific binding. Proteins were released from the beads by boiling for 5 minutes in Laemmli sample buffer (Sigma, St. Louis, MO). Following western blotting (see procedure below), band density readings from blots of cell lysates and pull-downs were obtained and used to generate a ratio of active to total Rac1, expressed as relative Rac1 activation. Ratios were subjected to Kruskal-Wallis analysis of variance (ANOVA) and Mann-Whitney U post hoc analysis with an α level of 0.05.

Western Blotting

Samples (20-40 µg lysates or entire pull-down sample) were run on 15% SDS-PAGE gels and transferred to nitrocellulose. Following blocking in 5% non-fat milk in tris buffered saline containing 0.1% Tween-20 (TBST) for 1 hour, membranes were incubated overnight at 4°C with rabbit anti Rac1 (Cell Signaling, Danvers, MA) primary antibody at a dilution of 1:500. Membranes were washed 3 times for 10 minutes each with TBST before incubation at room temperature with horseradish peroxidase (HRP)-conjugated secondary antibody (goat anti-rabbit 1:5,000; Invitrogen, Carlsbad, CA) for 2 hours. Following incubation, membranes were washed with TBST 3 times for 10 minutes each, followed by two 10-minute washes with Tris-buffered saline (TBS). Blots were then incubated with ChemiGlow enhanced luminescence reagent (Alpha Innotech, San Leandro, CA) for 5 minutes according to the manufacturer's suggestions, exposed to X-ray film, developed, and analyzed with the FluorChem HD2 Imaging System (Alpha Innotech, San Leandro, CA). Background subtracted band intensities were obtained using densitometry and integrating the area under the peak detected for each band.

Measurement of RhoA Activation by ELISA

RhoA activation in growth cones and whole cell lysates was analyzed using an ELISA-based activation kit (Rho G-LISA, Cytoskeleton, Denver, CO)

according to the manufacturer's instructions. Briefly, samples were prepared as described above and loaded with binding buffer (supplied with kit) onto a Rho-GTP affinity plate (which contains Rhotekin coated wells to bind active forms of RhoA) for a 30 minute incubation at 4°C. Each well was loaded with 30-50 µg total protein. The plate was washed with wash buffer to reduce non-specific binding and then incubated with a RhoA primary antibody (supplied with the kit) at room temperature for 45 minutes followed by incubation with an HRP-conjugated secondary antibody for 45 minutes. Following washing steps, the plate was incubated with HRP detection reagent for 15 minutes at 37°C. Reported absorbance (O.D.) readings at 490 nm were blank corrected by subtracting the absorbance of the blank sample (containing only lysis buffer) from the readings of each sample and represent the amount of active RhoA. Experiments were normalized by dividing the absorbance by the concentration of total protein used for that set of lysates. Kruskal-Wallis analysis of variance was used to test for main effects. Pairwise comparisons were made using Mann-Whitney U post hoc analyses with a significance level of $\alpha=0.05$

Localization of Actin Binding Proteins in Growth Cones

Treatment Groups

Immunocytochemistry was utilized to determine the effect of Rho GTPase activity on colocalization of the actin-binding proteins VASP, WAVE, Arp3 and profilin. Specifically, B35 cells, cultured on glass coverslips for 24 hours, were serum starved for 24 hours and then treated with 8-Br-cAMP (Sigma, St. Louis, MO), Y27632, Toxin A, or NSC23766 (EMD Biosciences, San Diego, CA). All treatments were carried out for 1 hour. There were 6 treatment groups as follows: SCM, SFM, 10 μ M 8-Br-cAMP, 100 μ M NSC23766, 10 ng/mL Toxin A, and 5 μ M Y27632.

Immunocytochemistry

Following treatment, cells were fixed in 4% paraformaldehyde for 20 minutes, washed with PBS, and blocked for 30 minutes with PBS containing 0.1% Triton X-100 and 1.5% pre-immune secondary-specific serum. The cells were incubated overnight at 4°C with the appropriate primary antibody at a 1:200 dilution in blocking buffer. Antibodies were rabbit anti-VASP (4 μ g/mL; Chemicon, Temecula, CA), rabbit anti-WAVE (2 μ g/mL; Upstate, Charlottesville, VA), rabbit anti-profilin at (1 μ g/mL; Cytoskeleton, Denver, CO) or rabbit anti-Arp3 (Upstate, Charlottesville, VA). Following two 5-minute washes in blocking

buffer, cells were incubated with secondary antibody (donkey anti rabbit AlexaFluor 555, 0.5 $\mu\text{g}/\text{mL}$, Invitrogen, Carlsbad, CA) in blocking buffer for 1 hour at room temperature. The dilution of 1:200 was bright enough to observe staining without incurring non-specific binding, as determined by omitting the primary antibody. After two more 5-minute washes, cells were double-labeled by a second incubation with a different mouse primary antibody overnight (either mouse anti Arp3, mouse anti profilin, mouse anti WAVE, or mouse anti VASP). All of the mouse primary antibodies were used at a dilution of 1:200 in blocking buffer and were obtained from BD Transduction Labs (Franklin Lakes, NJ). The procedure continued as described with donkey anti rabbit Alexa Fluor 488 (0.5 $\mu\text{g}/\text{mL}$; Invitrogen, Carlsbad, CA) as the secondary antibody. After the final washes, coverslips were mounted on slides with mounting medium (Vectashield, Vector Labs, Burlingame, CA) containing 4',6-diamidino-2-phenylindole (DAPI; stains double-stranded DNA). Coverslips were imaged through a 100X objective using Zeiss Axiovision imaging software and quantified by counting fluorescent localizations and co-localizations corresponding to the actin binding proteins (red, green or yellow puncta, no larger than 0.25 μm). This was done separately for the filopodial, lamellipodial, and central regions of the growth cones. For each treatment condition, the first quantifiable growth cone in each of 5 regions of the coverslip was analyzed for the number of localizations of each protein. Each region was scanned from upper left to lower right. The first growth cone

encountered in each region that was free of interference from other cells was used for the analysis. Thus, 5 growth cones per coverslip were analyzed. Each co-localization (WAVE/VASP, WAVE/Arp3, WAVE/profilin, Arp3/VASP, Arp3/profilin and VASP/profilin) was therefore analyzed in 5 growth cones in each treatment condition per experiment. Experimental replicates provided a total n of 10 growth cones per condition. For localization of single antigens (WAVE, Arp3, VASP and profilin), 3 coverslips per condition were labeled in each experiment (n = 15 growth cones for each). Experimental replicates provided a total n of 30 for each condition. The number of localizations and the number of co-localizations for each region of the growth cone was subjected to Kruskal-Wallis ANOVA and Mann-Whitney U post hoc analysis with an α level of 0.05. Image capture conditions including lamp intensity and exposure time were kept constant and fixed to allow comparison between experimental conditions.

Measurement of Complex Formation of Actin-Binding Proteins

Treatment Groups

Co-immunoprecipitation was utilized to determine if complexing of the actin binding proteins VASP, WAVE, and profilin is influenced by Rac1 and RhoA activity. B35 cells were seeded at 20,000/cm² in 6-well tissue culture plates, grown until 90% confluent, serum deprived for 24 hours and treated similarly to

the immunocytochemistry experiments. Cells were exposed to treatments which either activate (8-Br-cAMP) or inhibit (NSC23766 or Toxin A) Rac1 and to treatments which inhibit RhoA signaling (Y27632 or Toxin A). There were 6 treatment groups as follows: SCM, SFM, 10 μ M 8-Br-cAMP, 100 μ M NSC23766, 10 ng/mL Toxin A, and 5 μ M Y27632.

Co-immunoprecipitation

Cells were lysed on ice with IGEPAL CA-630 lysis buffer (1.0% IGEPAL CA-630, 1.5 mM EDTA, 25 mM Tris-HCl (pH=7.4), and 150 mM NaCl) containing protease inhibitors and the protein content analyzed via Pierce BCA protein assay. Samples (500 μ g of total protein) were incubated with rabbit anti WAVE (5 μ g, Upstate, Charlottesville, VA) or rabbit anti VASP (2 μ g, Chemicon, Temecula, CA) at 4°C overnight. The immunocomplex was captured by incubating the reaction mixture with TrueBlot Rabbit IgG beads (eBioscience, San Diego, CA) for 1 hour at room temperature on a rocking platform. The beads were washed twice for 1 minute each in IGEPAL CA-630 lysis buffer and the immunoprecipitated protein complexes were separated by resuspending the beads in Laemmli buffer and boiling for 10 minutes. The components of the protein complexes were then identified by Western blot analysis using primary antibodies against actin-binding proteins: rabbit anti VASP (4 μ g/mL; Chemicon, Temecula, CA); rabbit anti-WAVE (2 μ g/mL; Upstate, Charlottesville, VA); rabbit

anti profilin (1 $\mu\text{g}/\text{mL}$; Cytoskeleton, Denver, CO) or rabbit anti Arp3 (Upstate, Charlottesville, VA). All of the primary antibodies were used at a dilution of 1:500 in 5% non-fat milk blocking buffer. The western blots were processed as described above. HRP-conjugated goat anti rabbit IgG secondary antibody (1:5000) was used for cell lysate blots. TrueBlot anti rabbit IgG conjugated to HRP (1:1000) was used for blots on which immunoprecipitation samples were run. Blots were then incubated with ChemiGlow enhanced chemiluminescent reagent (Alpha Innotech, San Leandro, CA) for five minutes according to the manufacturer's suggestions, exposed to X-ray film, developed, and analyzed with the FluorChem HD2 Imaging System (Alpha Innotech, San Leandro, CA). Background subtracted band intensities were obtained by densitometry. Kruskal-Wallis analysis of variance was used to test for main effects. Pairwise comparisons were made using Mann-Whitney U post hoc analyses with a significance level of $\alpha=0.05$.

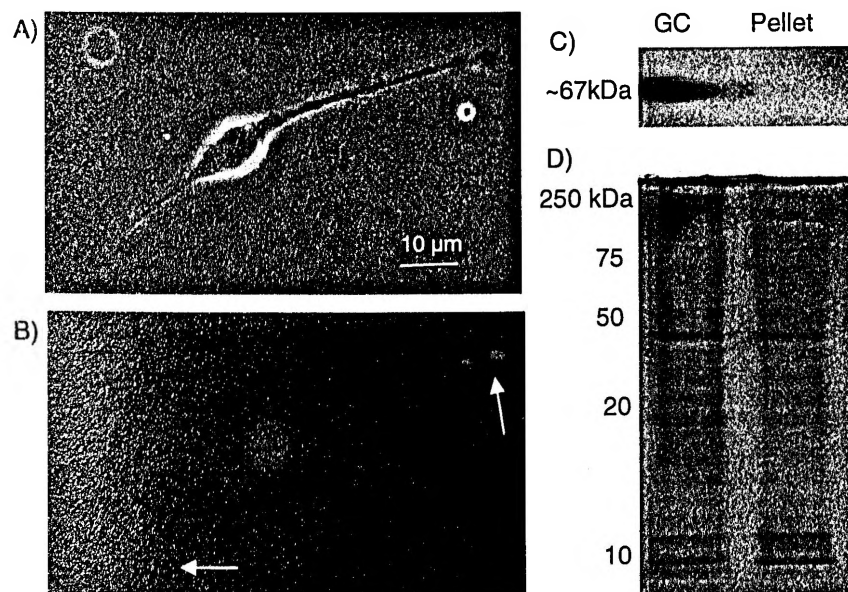
CHAPTER III

RESULTS

To determine differences in activation levels of Rac1 and RhoA in the growth cone and cell body regions of B35 rat neuroblastoma cells, we utilized a published growth cone fractionation procedure (Meyerson et al., 1992; Stettler et al., 1999). The protocol serves to separate growth cones from the rest of the cell using differential centrifugation on a sucrose gradient. Due to its lighter buoyant density, the growth cone fraction remains at the top of the sucrose gradient while the fraction containing the remainder of the cells is pelleted to the bottom. To ensure efficiency of the technique in our hands, an antibody to the growth cone marker, 2G13, was used to probe a western blot consisting of a sample recovered from the sucrose cushion/EDTA buffer interface and a sample collected from the pellet. This same antibody, along with an Alexa Fluor 488-conjugated secondary antibody, was used to label fixed B35 cells. Compared to a phase contrast image (Fig. 4A), anti-2G13 labeled only growth cones in B35 cells (Fig. 4B). Arrows indicate the position of the growth cones where immunolabeling is most intense. The corresponding Coomassie blue stained gel (Fig. 4D) showed sufficient protein for analysis was present in both fractions.

There was 1,104% more of the growth cone marker, 2G13, present in the sample collected from the top of the sucrose cushion than in the pelleted fraction (Fig. 4C). This was calculated as the difference between the ratios of the density of the band in the western blot to the sum of the densities of the bands for cytosolic proteins in the corresponding Coomassie-stained gel. The immunoreactive protein is approximately 67 kDa which corresponds to the reported molecular weight of 2G13 (Stettler et al., 1999). These studies indicated that the fractionation protocol yielded samples containing growth cones. Thus, the growth cone fractions were utilized for further studies.

Figure 4: Cell fractionation yields a fraction enriched for growth cones. Phase contrast (A) and corresponding fluorescence (B) images of B35 cells stained with the growth cone marker, anti-2G13 (green). Nuclei are labeled with DAPI (blue). Arrows indicate the position of the growth cone. Scale bar = 10 μm for both images. C) Western blot probed with anti-2G13. GC represents the fraction collected at the sucrose interface and pellet is the fraction migrating to the bottom of the tube, corresponding to the cell bodies. Comparison with the molecular weight standards indicates the immunoreactive protein is approximately 67 kDa. D) Coomassie blue stained gel of total proteins in the growth cone and pellet fractions.



Rac1 Activation Levels are Induced Within the Growth Cone

Rac1 activation has been shown to promote axon extension (Kuhn et al., 1999; Rashid et al., 2001). It is also known that the activation of Rac1 promotes membrane ruffling, which leads to outgrowth (Ridley et al., 2003). What has not been adequately studied is whether Rac1 activation is compartmentalized within the cell. To address this, we utilized pull-down assays and western blotting to compare activation levels in the whole cells to activation within the growth cone. A measurement of relative activation was calculated by dividing the amount of active Rac1 in a sample (from the pull-down assay) by the total amount of Rac1 for that sample (from the lysates blot).

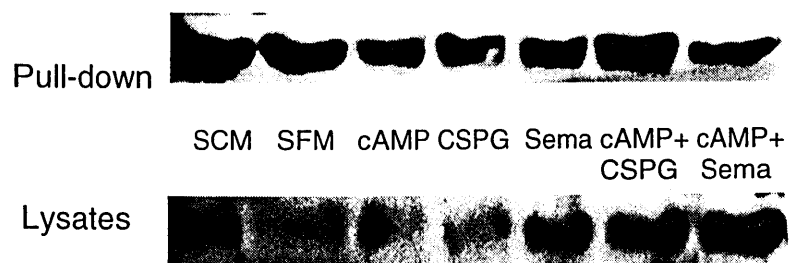
We first looked at Rac1 activation ratios in whole cell lysates, but found no significant differences between treatment groups including treatment with 8-Br-cAMP ($\chi^2 = 1.95$, $df = 5$, $p \leq 0.86$), which reportedly promotes neurite outgrowth (Otey et al., 2003; Schubert et al., 1974). Figure 5A shows the active Rac1, obtained by pull-down assay, as well as the total Rac1 in the whole cell lysates for each treatment (top blot). The graphical representation of the ratio of active Rac1 to total Rac1 is shown in Figure 5B.

We subsequently analyzed Rac1 activation in growth cone fractions. A representative pull-down blot showing active Rac1, as well as the total Rac1 in the growth cone fractions for each treatment is shown in Figure 5A (bottom blot).

In these experiments, Rac1 activation was increased (compared to SCM) by treatment with SFM and decreased (compared to SFM) by CSPGs. Kruskal-Wallis analysis showed the overall treatments to be significant ($\chi^2 = 12.25$, $df = 6$, $p \leq 0.05$). In these (and following experiments) where significance was achieved using the Kruskal-Wallis ANOVA, we made two sets of post-hoc comparisons using Mann-Whitney U pairwise test. First, we compared treatment of SFM to the baseline condition of cells in SCM. Second we compared outgrowth modulating treatments (8-Br-cAMP, CSPGs, Sema3A, and their combinations) to cells in SFM because these treatments were applied in SFM. Furthermore, combinatorial treatments were compared to 8-Br-cAMP alone, when included as a treatment condition. In this experiment, post-hoc comparisons revealed treatment with SFM ($p \leq 0.01$) reached significance when compared to cells maintained in SCM (Fig. 5B). Rac1 activation was not further increased by the presence of 8-Br-cAMP with SFM. Treatment with CSPGs reduced Rac1 activation compared to SFM ($p \leq 0.05$). Treatment which promotes outgrowth (SFM) of B35 cells increased Rac1 activation in the growth cones of B35 cells but not in whole cell lysates. CSPGs, which are inhibitory to outgrowth, decreased Rac1 activation in the growth cone. These results indicate that the changes in Rac1 activation within the growth cone were masked when analyzing whole cell lysates.

Figure 5: Rac1 activation in whole cell lysates and growth cone fractions. A) Representative pull-down (top blot) and lysates samples (bottom blot) from whole cell (WC) lysates probed for Rac1. B) Representative pull-down (top blot) and lysates samples (bottom blot) from growth cone (GC) fractions probed for Rac1. C) Graph represents the average activation ratio, normalized to SCM; n = 4 separate experiments for whole cell lysates and n = 3 for growth cone fractions (only two measurements were taken for Sema3A in the growth cone fraction; the range of the normalized activation ratio was 0.24 - 0.58). Error bars are SEM; * indicates a significant difference of SFM from SCM; # indicates significantly different from SFM, $p \leq 0.05$ (Kruskal-Wallis ANOVA, followed by Mann-Whitney U post-hoc).

A) WC



B) GC

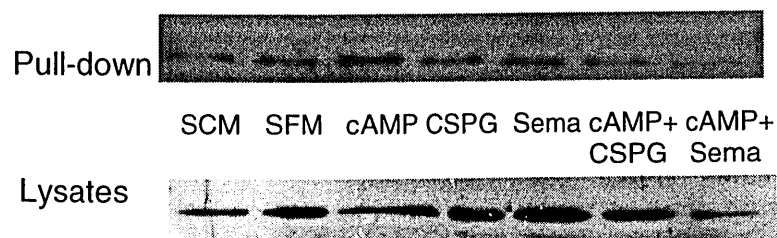
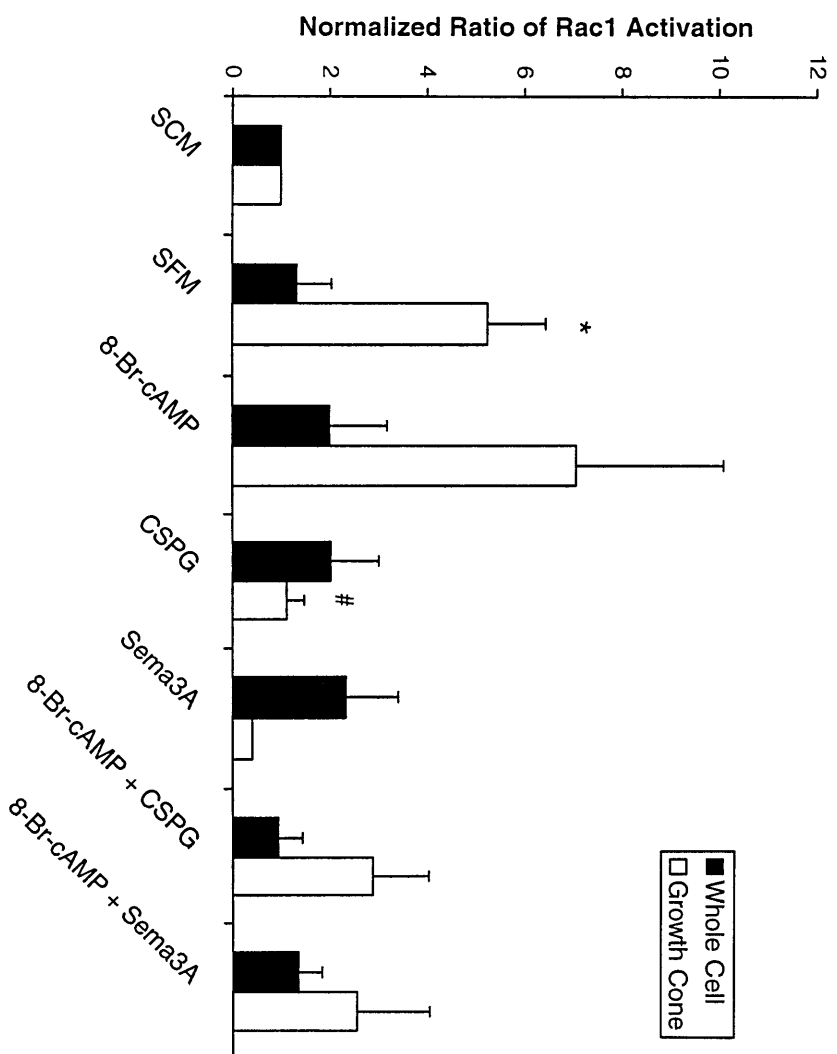


Figure 5 Continued

C)



RhoA Activation Levels are Induced Within the Cell Body and Growth Cones

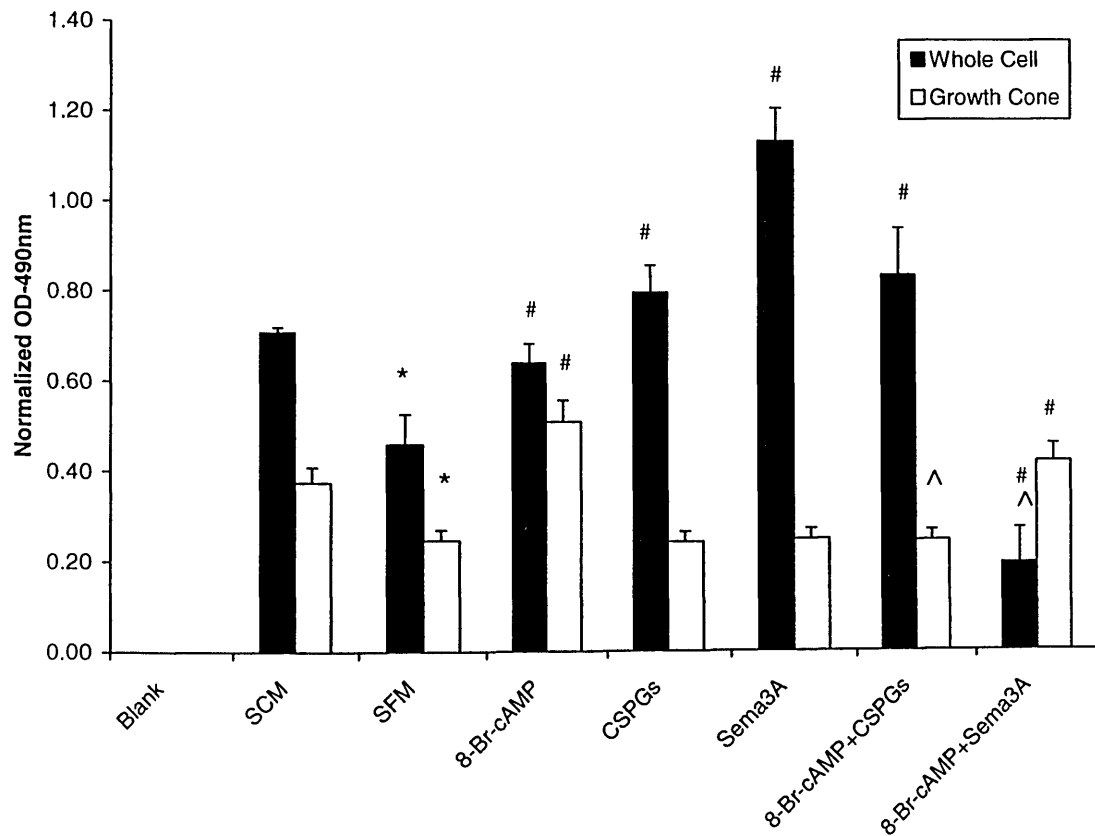
RhoA activation is associated with growth cone retraction and collapse (Kozma et al., 1997; Vastrik et al., 1999; Wahl et al., 2000), but it is unclear where in the cell regulation of activation states occurs. To measure changes in activation levels of RhoA in response to treatments which promote (SFM, 8-Br-cAMP) or inhibit (SCM, CSPGs, Sema3A) outgrowth, we utilized an ELISA-based assay designed to bind active (GTP-bound) forms of RhoA. These experiments were done in both whole cell lysates and growth cone fractions. The intensity of the absorbance of each sample at 490 nm correlates positively with the amount of active RhoA.

Significant responses to treatments were seen in the whole cell lysates. Following a significant Kruskal-Wallis analysis ($\chi^2 = 17.21$, $df = 6$, $p \leq 0.01$), treatment groups were subjected to Mann-Whitney U pairwise comparisons. Compared to cells in SCM, treatment with SFM ($p \leq 0.05$) significantly decreased RhoA activity (Fig. 6). Compared to SFM, all treatments except Sema3A in the presence of 8-Br-cAMP increased RhoA activation ($p \leq 0.05$ for all). Conversely, Sema3A with 8-Br-cAMP decreased RhoA activation ($p \leq 0.05$) compared to SFM. Furthermore, the addition of Sema3A to 8-Br-cAMP significantly reduced RhoA activation compared to 8-Br-cAMP alone ($p \leq 0.05$). Thus, the combination

of the two treatments inhibits the activation of RhoA observed by each independent treatment.

Similarly, a significant Kruskal-Wallis ($\chi^2 = 16.13$, $df = 6$, $p \leq 0.01$) prompted Mann-Whitney U pairwise comparisons of RhoA activation levels in B35 growth cones. Compared to SCM, SFM decreased RhoA activation ($p \leq 0.05$) (Fig. 6). Conversely, when compared to SFM, 8-Br-cAMP alone and with Sema3A both increased RhoA activation in growth cones ($p \leq 0.05$). Interestingly, the combination of 8-Br-cAMP with CSPGs decreased RhoA activation compared to 8-Br-cAMP alone ($p \leq 0.05$). These results differ from those observed in whole cell lysates where all but one of the drugs increased RhoA activation. These data may indicate that while RhoA activity is induced both in the cell body and growth cone, the signaling pathways or regulation of activation may be compartmentalized. Treatments that promote outgrowth (SFM) decreased RhoA activation while those that inhibit outgrowth increased RhoA activation in the cell body.

Figure 6: RhoA activation in B35 whole cell lysates and growth cone fractions. Graphs represent the average absorbance of each whole cell lysate (A) or growth cone sample (B) at 490nm, normalized by dividing each absorbance by the protein concentration used for that experiment. Data are means \pm standard error of the mean for 3 experiments. * indicates a significant difference from the serum containing media treatment (SCM); # indicates a significant difference from the serum free media treatment (SFM); ^ indicates a significant difference from 8-Br-cAMP, $p \leq 0.05$ (Kruskal-Wallis ANOVA, followed by Mann-Whitney U post-hoc).



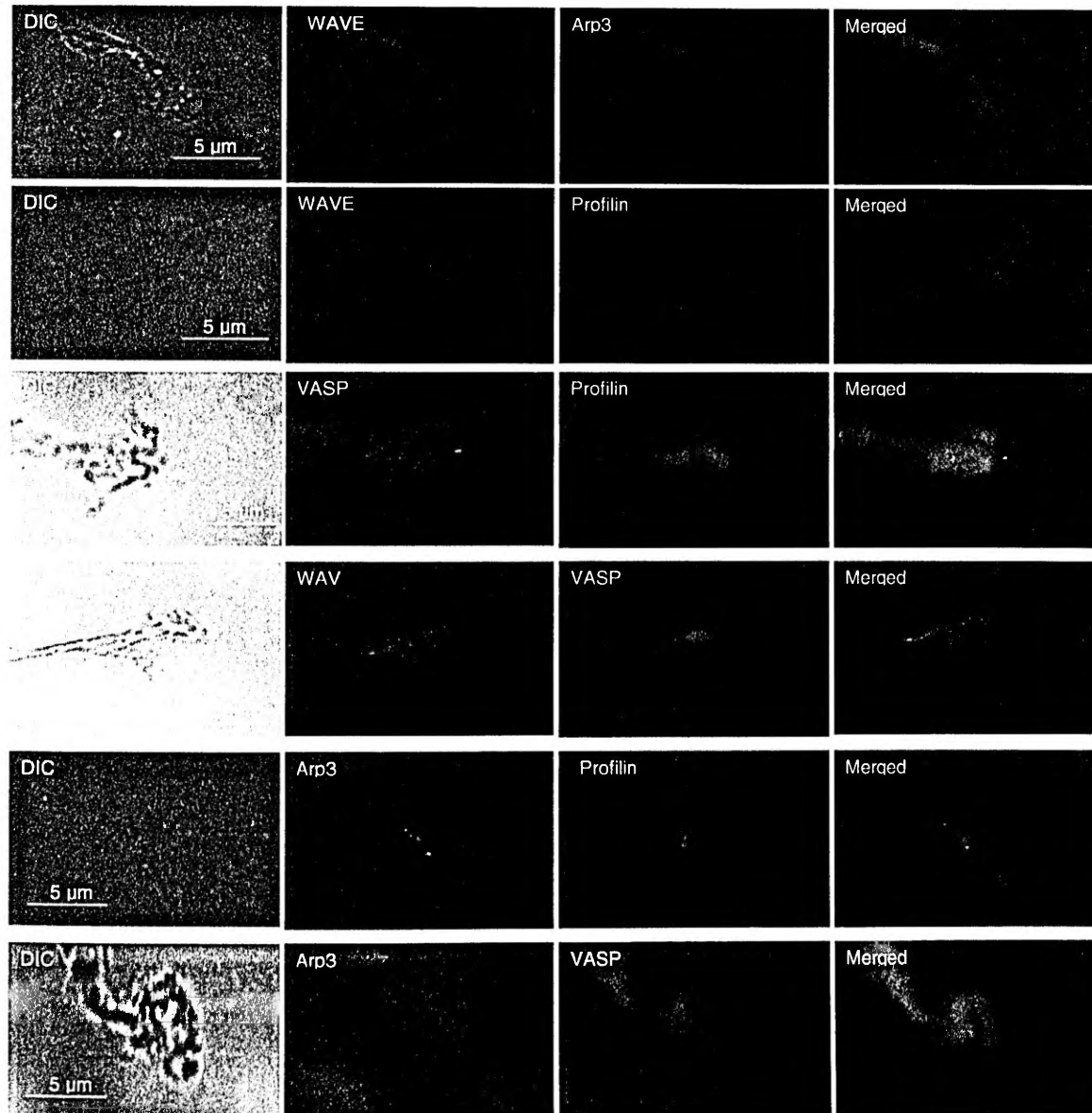
Actin Binding Proteins Localize to the Growth Cone When Treated with Rho GTPase Signaling Modulators

To determine what changes in the localization of the actin binding proteins, WAVE, VASP, Arp3, and profilin, occur in response to treatments which either activate (8-Br-cAMP) or inhibit (NSC23766 or Toxin A) Rac1 and to treatments which inhibit RhoA (Toxin A) or its signaling (Y27632, inhibits Rho kinase), we utilized immunocytochemistry techniques. Images (100X) of fluorescently labeled cells were quantified by counting fluorescent localizations corresponding to the actin binding proteins in the filopodial, lamellipodial, and central regions of the growth cones. Representative images of growth cones in 8-Br-cAMP are shown in Figure 7.

Figure 7: Co-localization of actin binding proteins in growth cones.

Representative 100X DIC images of the growth cone, individual channel images, and merged fluorescence immunolabeling of B35 cells in 8-Br-cAMP treatment.

Scale bar = 5 μ m. Note that all proteins co-localize within the growth cone.



In general, changes were observed in the localization of actin binding proteins in the filopodial, lamellipodial and central regions of B35 growth cones in response to both activating and inhibiting treatments. Specifically, when compared to SCM, Arp3 localization in the filopodia increased ($\chi^2 = 33.16$, $df = 5$, $p \leq 0.0001$) in response to the outgrowth-promoting treatment SFM ($p \leq 0.006$). Following comparison of localization of Arp3 after treatment with SFM alone and with the Rho GTPase modulating compounds, we found that Toxin A ($p \leq 0.001$) and Y27632 ($p \leq 0.002$) decreased Arp3 localization in the filopodia. Within the lamellipodia, 8-Br-cAMP ($p \leq 0.0001$) and NSC23766 (0.02) increased the number of immunopositive puncta while Toxin A decreased it ($p \leq 0.001$). The number of immunopositive puncta for Arp3 in the central region of the growth cone was decreased by Toxin A treatment as compared to SFM ($p \leq 0.0001$) (Fig. 8).

Results were very similar for the other actin binding proteins. For VASP, lamellipodial number of immunopositive puncta ($\chi^2 = 59.80$, $df = 5$, $p \leq 0.0001$) increased in response to the outgrowth promoting treatment, SFM ($p \leq 0.0001$) compared to SCM. Within the central region ($\chi^2 = 36.92$, $df = 5$, $p \leq 0.0001$), VASP was again increased by SFM ($p \leq 0.03$) (Fig. 9). When compared to SFM treatment, Toxin A ($p \leq 0.001$) and Y27632 ($p \leq 0.0001$) decreased VASP immunopositive puncta in the filopodia. Similarly, VASP immunopositive puncta in the lamellipodia was decreased by the Rho GTPase signaling inhibitors (Toxin

A, $p \leq 0.0001$; NSC23766, $p \leq 0.03$; Y27632, $p \leq 0.0001$). In the central region of the growth cone, the same trend continued, showing a decrease in the number of immunopositive puncta upon treatment with Toxin A ($p \leq 0.0001$) and Y27632 ($p \leq 0.0001$) (Fig. 9).

Figure 8: Arp3 localization in B35 growth cone regions. Data are means \pm SEM, n = 30; * indicates a significant difference from SCM and # indicates a significant difference from SFM, at $p \leq 0.05$ (Mann-Whitney U post-hoc following Kruskal-Wallis ANOVA).

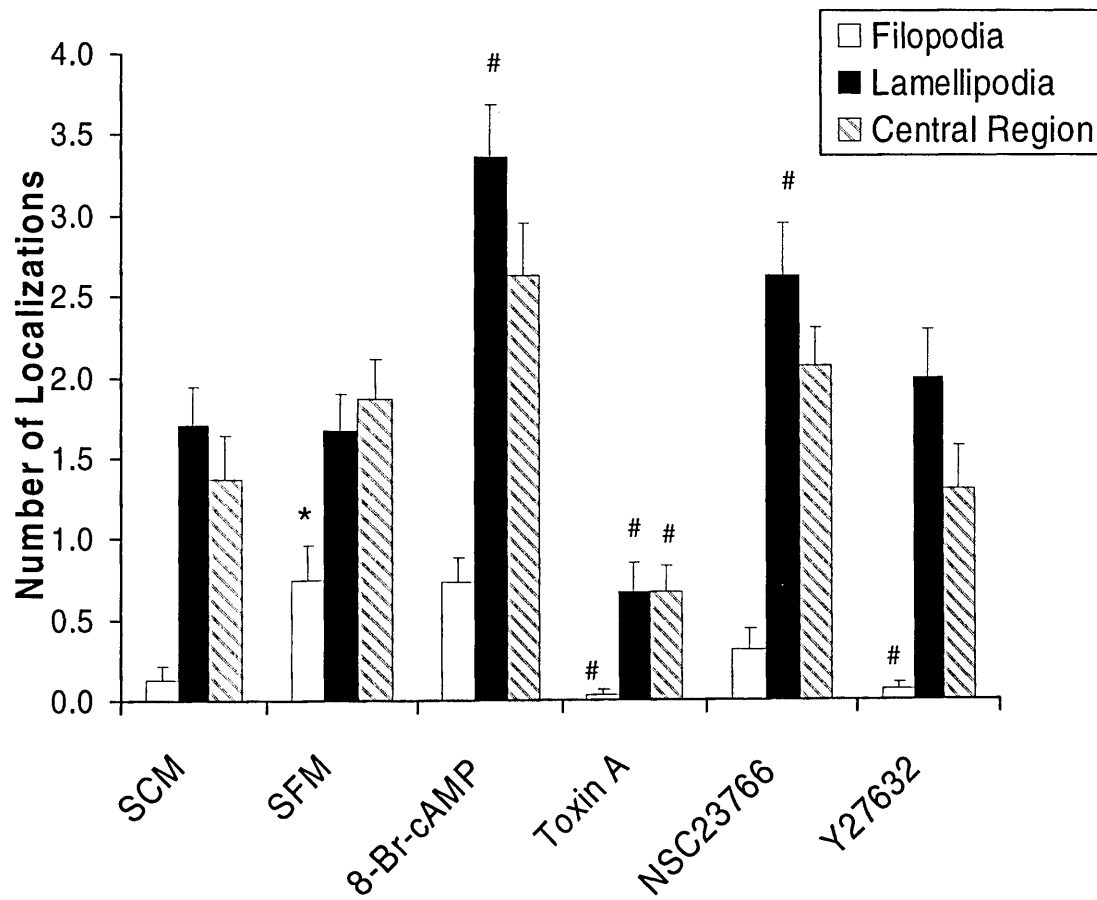
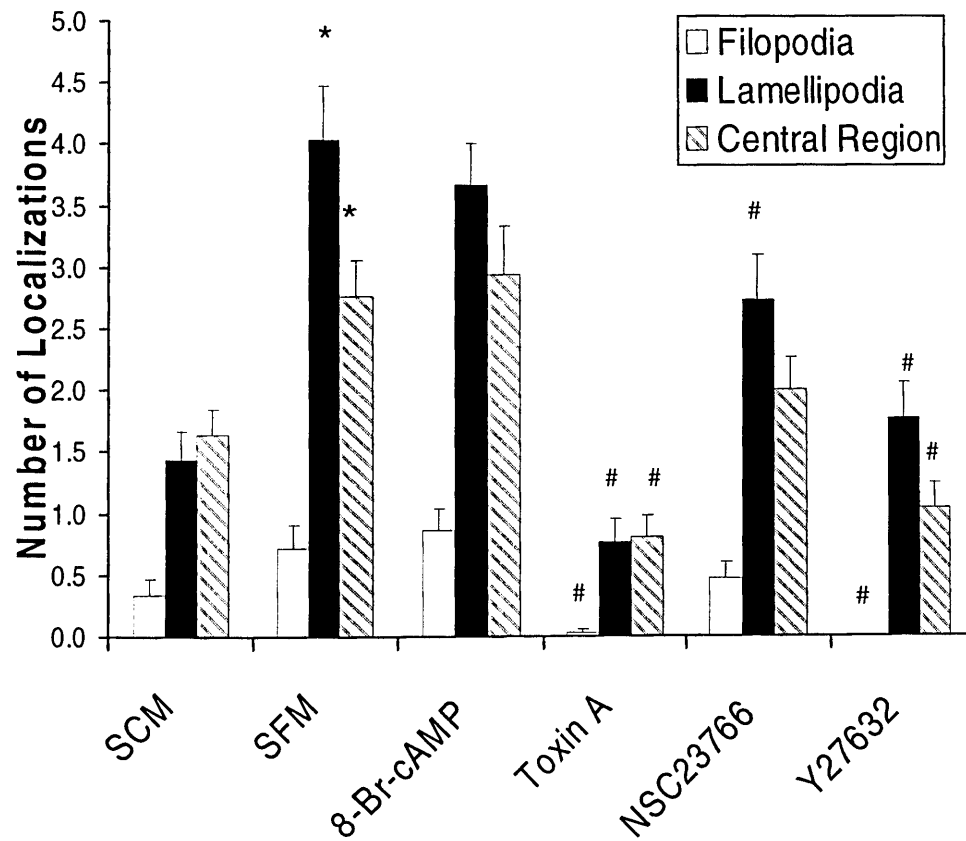


Figure 9: VASP localization in B35 growth cone regions. Data are means \pm SEM, n = 30; * indicates a significant difference from SCM and # indicates a significant difference from SFM, at $p \leq 0.05$ (Mann-Whitney U post-hoc following Kruskal-Wallis ANOVA).



Consistent with results from the other actin binding proteins, the number of immunopositive puncta for WAVE in the filopodia ($\chi^2 = 38.75$, $df = 5$, $p \leq 0.0001$) increased with outgrowth promoting treatment compared to SCM (SFM, $p \leq 0.0001$). Lamellipodial number of WAVE immunopositive puncta ($\chi^2 = 36.67$, $df = 5$, $p \leq 0.0001$) also increased compared to SCM with treatment of SFM ($p \leq 0.006$). When comparing the treatments to SFM alone, Toxin A ($p \leq 0.0001$), NSC23755 ($p \leq 0.01$) and Y27632 ($p \leq 0.0001$) all decreased the WAVE number of immunopositive puncta in the filopodial region. Within the lamellipodia, the number of WAVE immunopositive puncta decreased in response to Toxin A treatment ($p \leq 0.0001$) compared to SFM. Toxin A ($p \leq 0.0001$), NSC23766 ($p \leq 0.04$) and Y27632 ($p \leq 0.002$) all decreased the number of immunopositive puncta in the central region ($\chi^2 = 35.89$, $df = 5$, $p \leq 0.0001$) compared to SFM (Fig. 10).

As seen with the other proteins, the number of profilin immunopositive puncta in the filopodia was increased, compared to SCM ($\chi^2 = 32.95$, $df = 5$, $p \leq 0.0001$), by treatment which promotes outgrowth (SFM, $p \leq 0.03$). Within the lamellipodia ($\chi^2 = 30.36$, $df = 5$, $p \leq 0.0001$) the number of profilin immunopositive puncta were also increased by treatment with SFM ($p \leq 0.02$). Within the central region ($\chi^2 = 27.41$, $df = 5$, $p \leq 0.0001$), SFM increased the number of profilin immunopositive puncta ($p \leq 0.03$) (Fig. 11).

Figure 10: WAVE localization in B35 growth cone regions. Data are means \pm SEM, n = 30; * indicates a significant difference from SCM and # indicates a significant difference from SFM, at $p \leq 0.05$ (Mann-Whitney U post-hoc following Kruskal-Wallis ANOVA).

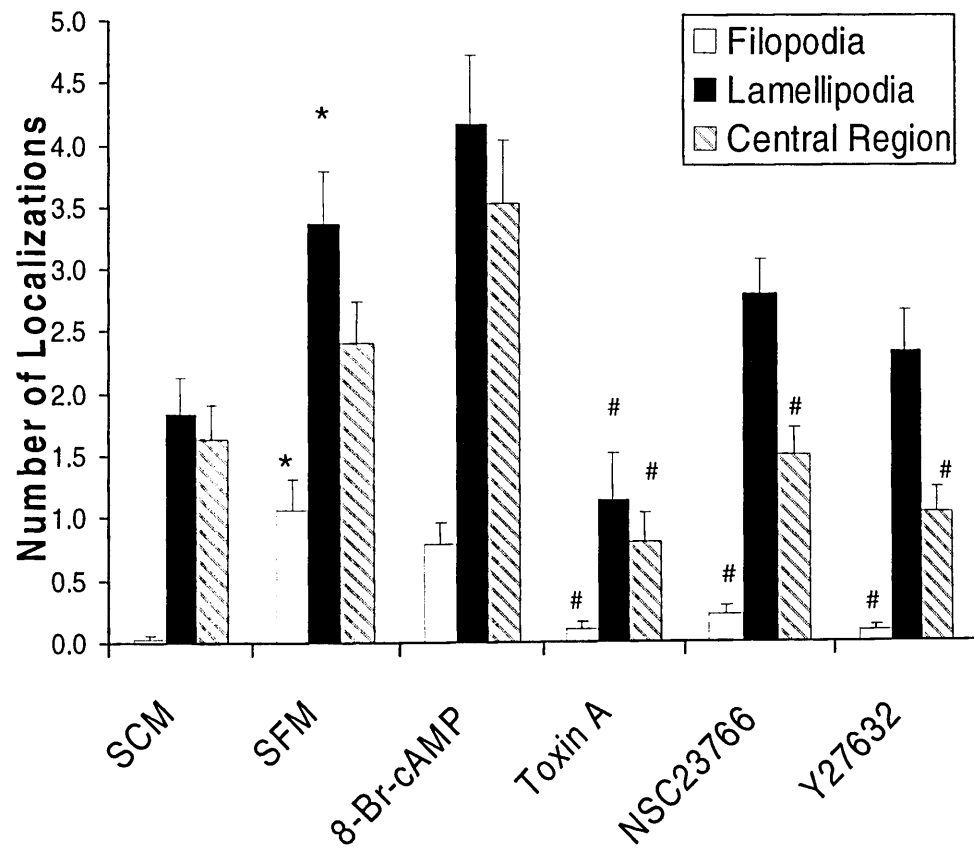
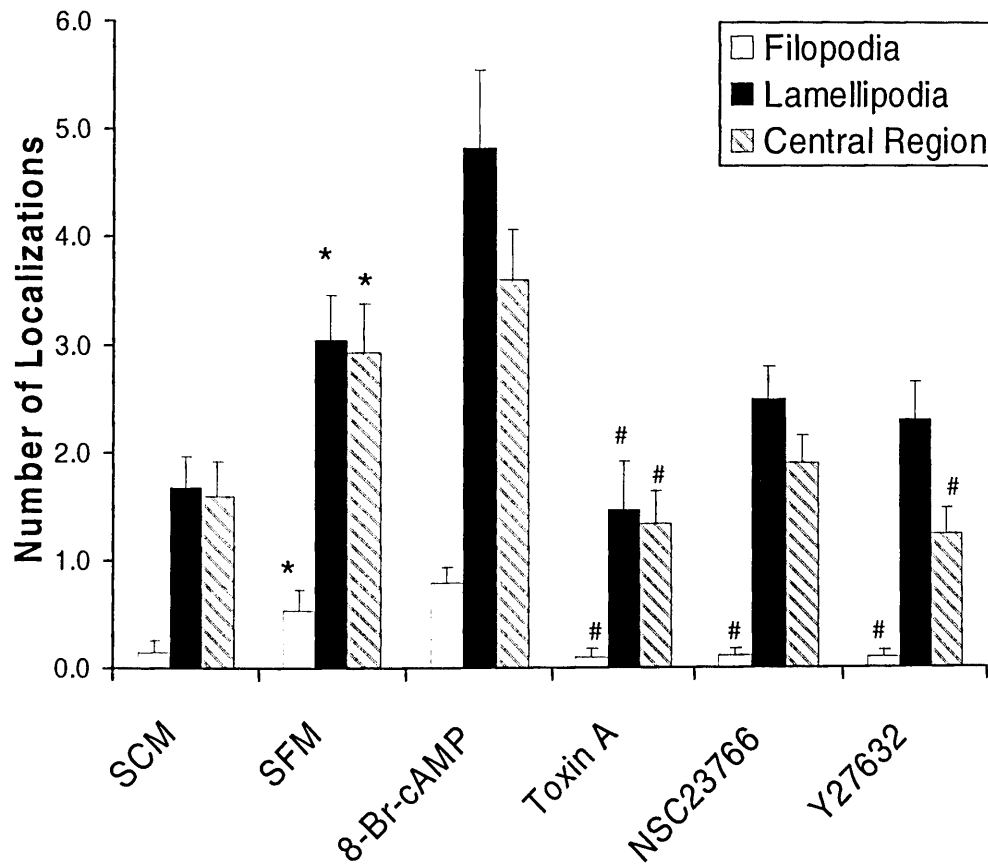


Figure 11: Profilin localization in B35 growth cone regions. Data are means \pm SEM, n = 30; * indicates a significant difference from SCM and # indicates a significant difference from SFM, at $p \leq 0.05$ (Mann-Whitney U post-hoc following Kruskal-Wallis ANOVA).



When comparing treatments to SFM alone, Toxin A, NSC23766, and Y27632 all decreased the number of profilin immunopositive puncta in the filopodia ($p \leq 0.01$, 0.03, and 0.03, respectively). In the lamellipodia as well, Toxin A decreased the number of immunopositive puncta of profilin compared to SFM ($p \leq 0.002$). Similar effects were seen in the central region, where Toxin A ($p \leq 0.005$) and Y27632 ($p \leq 0.005$) both decreased the number of profilin immunopositive puncta compared to SFM alone (Fig. 11).

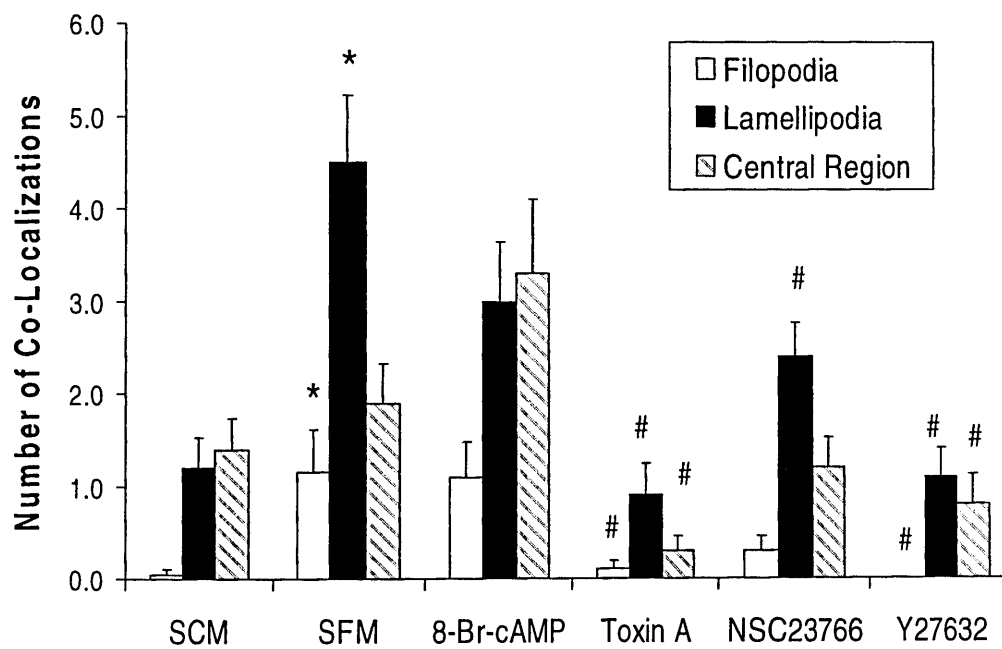
In summary, treatments which increase neurite outgrowth also increase the number of immunopositive puncta for actin binding proteins to the filopodial, lamellipodial and central regions of B35 growth cones. In general, inhibition of both Rac1 and RhoA by Toxin A treatment decreased the number of actin binding protein immunopositive puncta to all three regions of the growth cone. Treatment with Y27632 (an inhibitor to RhoA signaling) decreased this number compared to SFM (bringing localization levels back down to baseline levels seen in cells in SCM). NSC23766 treatment (a Rac1 inhibitor) sometimes resulted in a surprising increase in the number of actin binding protein immunopositive puncta. Taken together with results from the GTPase activation assays, these data indicate that activation of Rac1 and RhoA in growth cones may contribute to changes in the localization of actin binding proteins.

Co-localization of Actin Binding Proteins Within the Growth Cone Increases When Treated with Rho GTPase Modulators

To determine levels of co-localization of actin binding proteins, we analyzed 100X fluorescence images (see representative images in Fig. 7). Areas of co-localization (yellow) were quantified from the merged images for the filopodial, lamellipodial, and central regions of the growth cone. In general, changes in the co-localization of the actin binding proteins were similar to the changes observed in the localization of single proteins. Specifically, WAVE and VASP co-localization within the filopodia ($\chi^2 = 16.52$, $df = 5$, $p \leq 0.006$) increases in response to outgrowth promoting treatments as compared to SFM ($p \leq 0.04$). This same treatment also increased WAVE and VASP co-localization in the lamellipodial region ($\chi^2 = 26.26$, $df = 5$, $p \leq 0.0001$) (SFM, $p \leq 0.0001$) (Fig. 12).

When treated with Toxin A, WAVE and VASP co-localization decreased in the filopodia compared to SFM ($p \leq 0.05$) or Y27632 ($p \leq 0.01$). Toxin A ($p \leq 0.0001$), NSC23766 ($p \leq 0.01$), and Y27632 ($p \leq 0.0001$) all decreased in the lamellipodia compared to SFM. Similarly, in the central region, co-localization of WAVE and VASP decreased in response to Toxin A ($p \leq 0.02$) and Y27632 ($p \leq 0.04$) (Fig. 12).

Figure 12: Co-localization of WAVE and VASP. Data are means \pm SEM, n = 10; * indicates a significant difference compared to SCM while # indicates a significant difference compared to SFM for that region of the growth cone, $p \leq 0.05$ (Kruskal-Wallis ANOVA and Mann-Whitney U post-hoc).



Analysis of the co-localization of VASP and profilin revealed the same trend, though not many of the changes were significant. Toxin A ($p \leq 0.01$) and Y27632 ($p \leq 0.04$) both decreased co-localization compared to SFM in the lamellipodia ($\chi^2 = 19.31$, $df = 5$, $p \leq 0.002$) while only Y27632 ($p \leq 0.006$) had the same effect in the central region ($\chi^2 = 13.52$, $df = 5$, $p \leq 0.019$) (Fig. 13).

WAVE and profilin co-localization did not change significantly in the filopodia in response to our treatments. Within the lamellipodia ($\chi^2 = 17.27$, $df = 5$, $p \leq 0.004$) and central region ($\chi^2 = 17.9$, $df = 5$, $p \leq 0.003$), co-localization of WAVE and profilin increased in response to 8-Br-cAMP (lamellipodia, $p \leq 0.02$; central region, $p \leq 0.02$) as compared to SFM (Fig. 14).

Within the filopodial region of the growth cone ($\chi^2 = 14.21$, $df = 5$, $p \leq 0.01$), WAVE and Arp3 co-localization increased as compared to SCM when the cells were placed in SFM ($p \leq 0.013$). The co-localization of WAVE and Arp3 in the SFM treatment decreased in the filopodial, lamellipodial ($\chi^2 = 13.84$, $df = 5$, $p \leq 0.017$) and central regions ($\chi^2 = 14.98$, $df = 5$, $p \leq 0.011$) of the growth cone when Toxin A was added (filopodia, $p \leq 0.01$; lamellipodia, $p \leq 0.03$; central region, $p \leq 0.005$). NSC23766 ($p \leq 0.05$) and Y27632 ($p \leq 0.04$) also decreased co-localization in the filopodia compared to SFM (Fig. 15).

Figure 13: Co-localization of VASP and profilin. Data are means \pm SEM, n = 10; * indicates a significant difference compared to SCM while # indicates a significant difference compared to SFM for that region of the growth cone, $p \leq 0.05$ (Kruskal-Wallis ANOVA and Mann-Whitney U post-hoc).

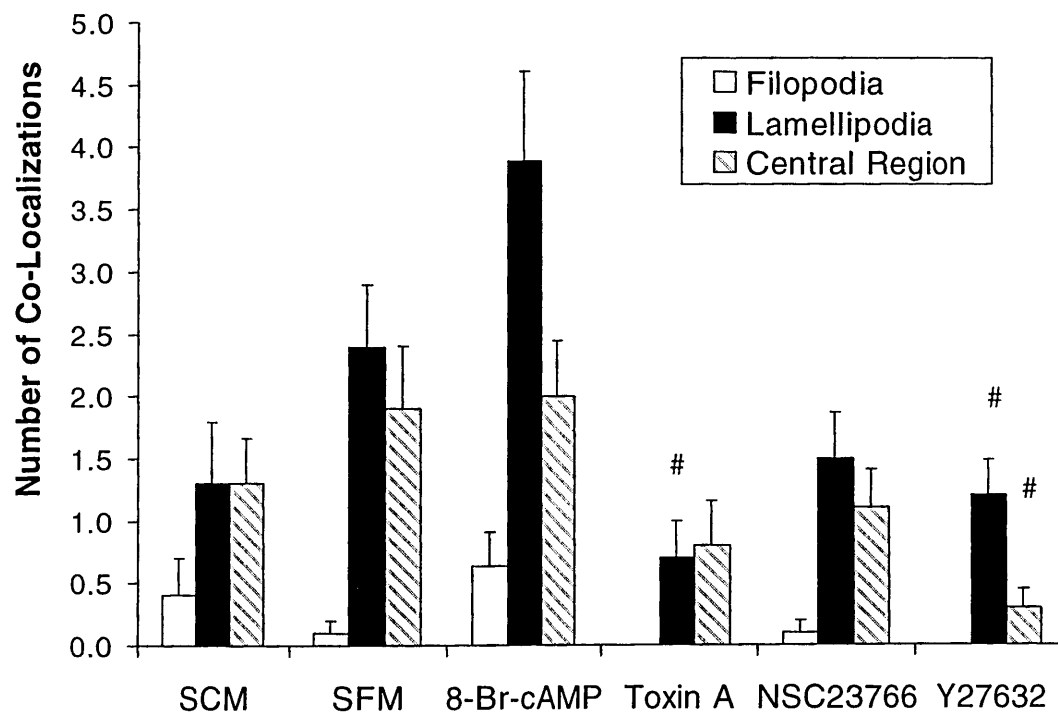


Figure 14: Co-localization of WAVE and profilin. Data are means \pm SEM, n = 10; * indicates a significant difference compared to SCM while # indicates a significant difference compared to SFM for that region of the growth cone, $p \leq 0.05$ (Kruskal-Wallis ANOVA and Mann-Whitney U post-hoc).

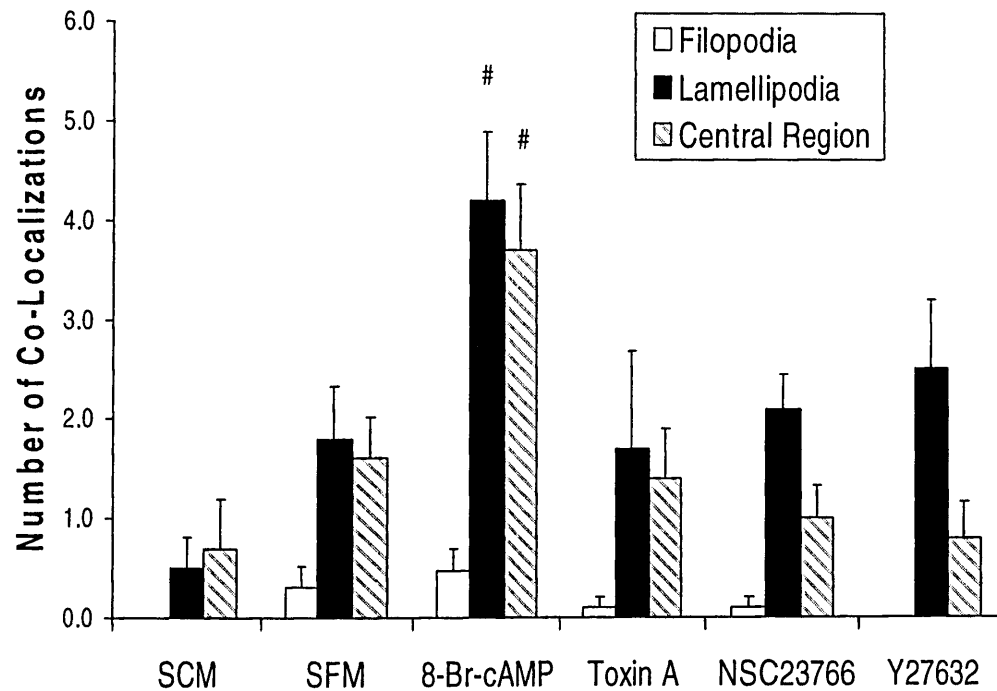
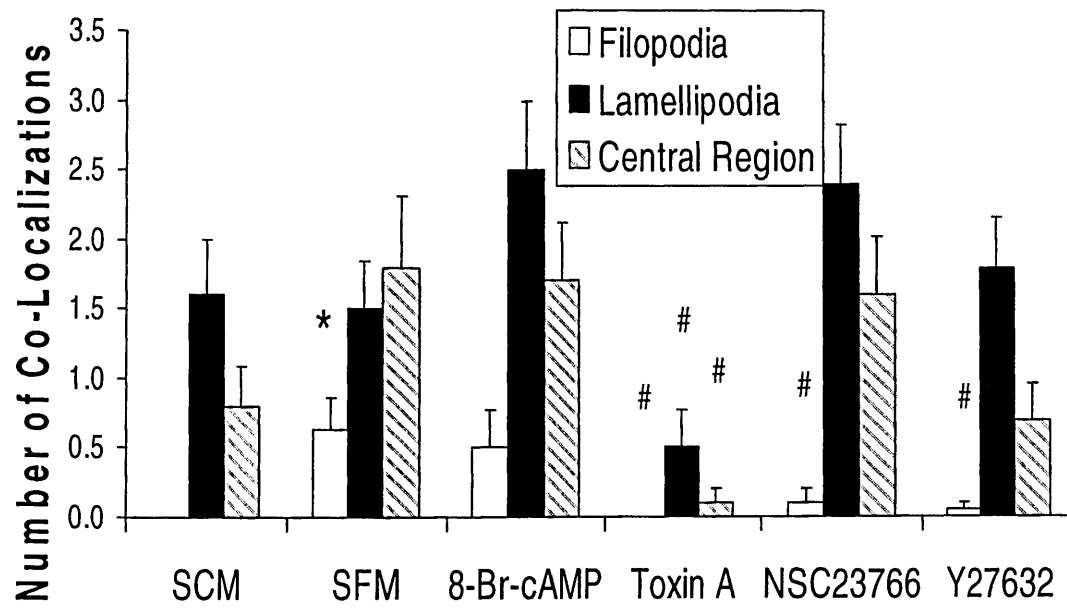


Figure 15: Co-localization of WAVE and Arp3. Data are means \pm SEM, n = 10; * indicates a significant difference compared to SCM while # indicates a significant difference compared to SFM for that region of the growth cone, $p \leq 0.05$ (Kruskal-Wallis ANOVA and Mann-Whitney U post-hoc).



Arp3 and profilin co-localization increased in the central region ($\chi^2 = 22.71$, $df = 5$, $p \leq 0.0001$) following treatment with SFM ($p \leq 0.02$) as compared to SCM. Y27632 decreased co-localization of Arp3 and profilin as compared to SFM within the central region ($p \leq 0.002$) (Fig. 16).

Though no significant changes were observed in the co-localization of Arp3 and VASP in the filopodia as compared to SCM, co-localization was increased in the lamellipodia ($\chi^2 = 25.98$, $df = 5$, $p \leq 0.0001$) by treatment with SFM ($p \leq 0.007$). A response was observed in the lamellipodial and central regions ($\chi^2 = 19.31$, $df = 5$, $p \leq 0.002$) in response to Toxin A and Y27632 as compared to SFM. Treatment with Toxin A decreased co-localization in all three areas of the growth cone compared to SFM (filopodia, $p \leq 0.01$; lamellipodia, $p \leq 0.001$; central region, $p \leq 0.001$). Y27632 had the same effect (filopodia, $p \leq 0.01$; lamellipodia, $p \leq 0.04$; central region, $p \leq 0.05$) (Fig. 17).

These results indicate, much like the analysis of the localization of single actin binding proteins, that treatments which promote outgrowth (SFM and 8-Br-cAMP) increase the co-localization of Arp3, VASP, WAVE and profilin. This increase in co-localization is observed in the filopodia, lamellipodia, and central region of the growth cone. While treatments which inhibited RhoA and Rac1 (Toxin A) and RhoA signaling (Y27632) generally did not increase and sometimes decreased co-localization of the actin binding proteins, the Rac1 inhibitor alone (NSC23766)

frequently increased co-localization. Although Rac1 was inhibited by this treatment, Cdc42 was still active in promoting actin polymerization. Furthermore, the inhibition of Rac1 may have resulted in lower levels of active RhoA. This would also lead to an increase in actin polymerization and may explain the increase in localization of actin binding proteins to the growth cone.

Figure 16: Co-localization of Arp3 and profilin. Data are means \pm SEM, n = 10; * indicates a significant difference compared to SCM while # indicates a significant difference compared to SFM for that region of the growth cone, $p \leq 0.05$ (Kruskal-Wallis ANOVA and Mann-Whitney U post-hoc).

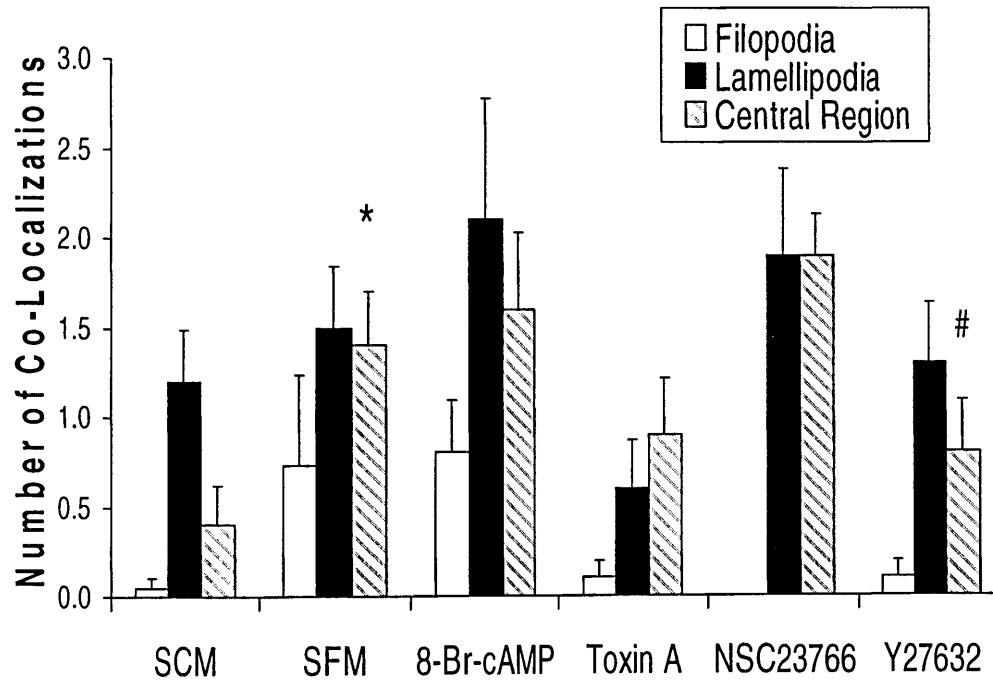
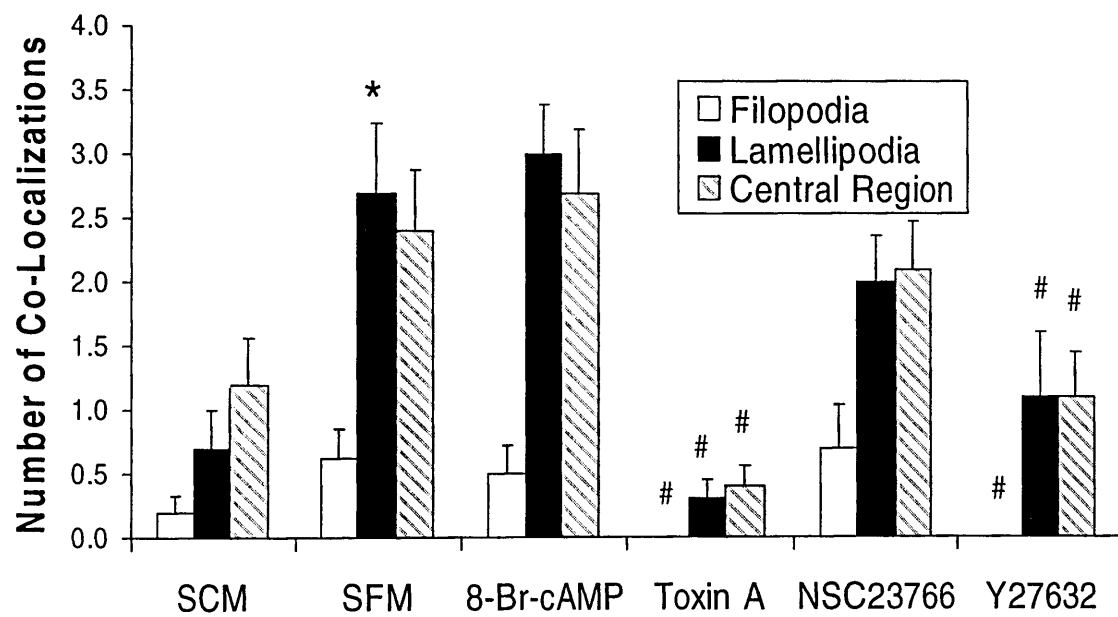


Figure 17: Co-localization of Arp3 and VASP. Data are means \pm SEM, n = 10; * indicates a significant difference compared to SCM while # indicates a significant difference compared to SFM for that region of the growth cone, p \leq 0.05 (Kruskal-Wallis ANOVA and Mann-Whitney U post-hoc).



Arp3 Binds to WAVE and VASP, but Profilin Only Binds to VASP

Previous studies have shown that changes in actin dynamics involve many proteins with varying roles and that many of these proteins work in complexes with one another to carry out their functions (Schmidt et al., 1995; Meyer and Feldman, 2002). Following our immunocytochemistry assays which showed that many of these proteins co-localize in the growth cone, we wanted to test whether these actin binding proteins form complexes with one another and if the complex is affected by treatments that change activation levels of Rac1 and RhoA.

To test this, we performed a series of co-immunoprecipitation assays. Following treatments as described for the immunocytochemistry analysis, VASP and WAVE were immunoprecipitated. We chose these two proteins because they are associated with actin polymerization either nucleated as side chains (WAVE) or from barbed ends (VASP). The samples were analyzed by western blotting using Arp3 and profilin as probes.

Each experiment was run with a negative control sample which contained only cell lysates and rabbit IgG beads (no precipitating antibody) to ensure proteins are binding specifically to the antibody rather than to the beads themselves. We also performed a negative control experiment using rabbit IgG in place of the precipitating antibody to be sure that any bands observed at 50

kDa were the result of our protein of interest rather than the heavy chain of the precipitating antibody (Fig. 18). The TrueBlot Co-IP kit used is designed to limit heavy chain interference. 3T3/A31 cell lysates (20 µg; Upstate, Charlottesville, VA) were run as a positive control to ensure any negative results were not due to blotting errors. Successful immunoprecipitations were confirmed by western blotting for the immunoprecipitated protein (data not shown).

We found that WAVE associates with Arp3. The blot containing the lysates samples indicates that Arp3 content is fairly constant across all samples (Fig. 19, lysates). The co-immunoprecipitate blot, probed for Arp3, shows that WAVE associates with Arp3 (Fig. 19, IP). We compared band intensity between treatments and found no significant differences between treatment groups ($\chi^2 = 5.05$, $df = 5$, $p \leq 0.41$) (Fig. 19B). These results indicate that although co-localization of actin binding proteins is modulated by changes in Rho GTPase activation, that co-localization does not necessarily lead to an increase in complex formation.

Figure 18: Negative control blot to ensure limited interference from the heavy chain of the precipitating antibody. 3T3 and B35 cell lysates were loaded as positive controls. The rabbit IgG sample was immunoprecipitated with 5 μ g of rabbit IgG in place of the 5 μ g of VASP antibody used in the VASP IP sample. The blot was probed for Arp3.

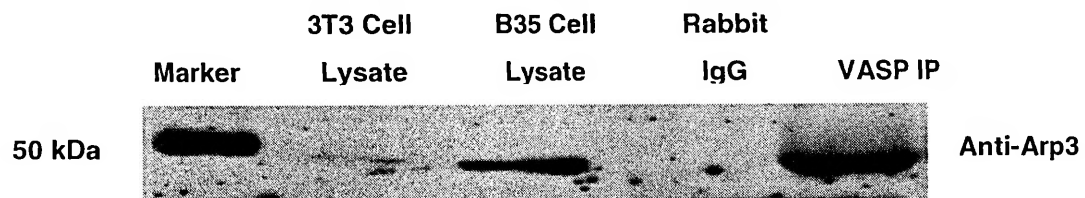
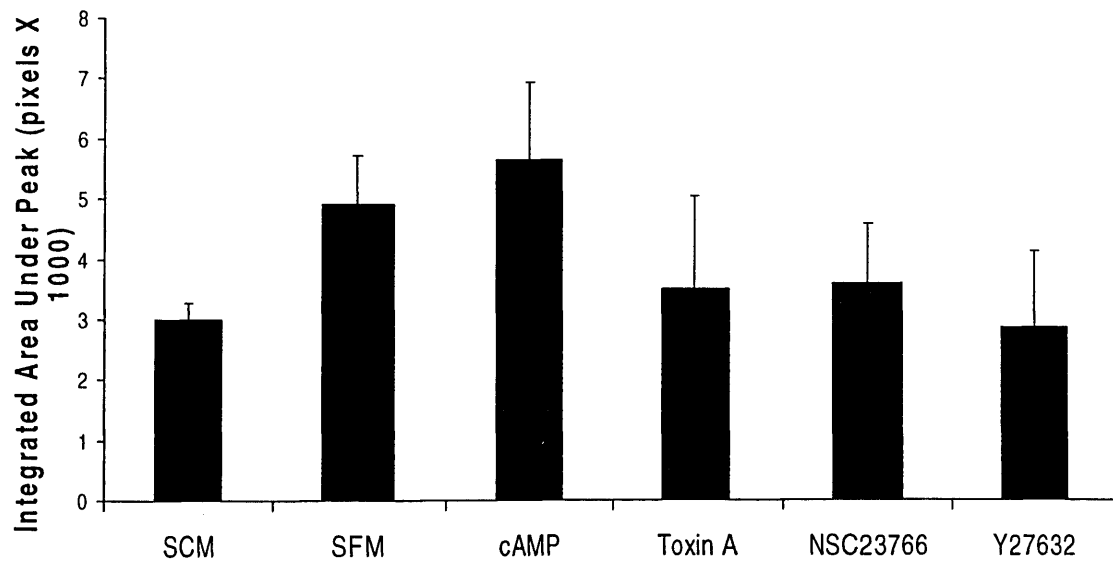
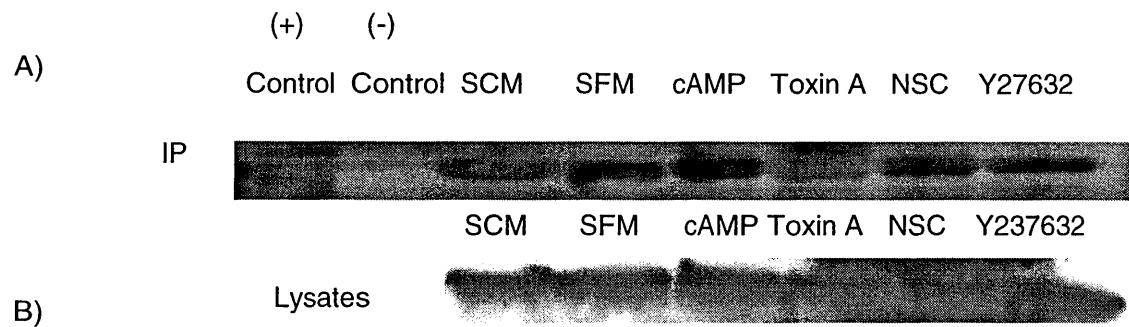


Figure 19: WAVE binds to Arp3. The blots depict either cell lysates (A, bottom blot) or samples subjected to the immunoprecipitation protocol (A, top blot). Both blots were probed for Arp3 (~50 kDa). The graph represents average band intensities \pm SEM; n = 3 separate experiments (B).



The WAVE IP blots were also probed for profilin. Again, profilin content appears to be even across treatment conditions (Fig. 20, lower blot). In this case, WAVE does not associate with profilin as shown by the IP blot (Fig. 20, top blot). The presence of profilin in the positive control sample demonstrates that the blotting process was successful.

We performed these same assays using anti-VASP as the precipitating antibody. We observed that VASP binds to Arp3 (Fig. 21, IP blot). We compared band intensity between treatments and, again, found no significant differences between treatment groups ($X^2 = 7.93$, $df = 5$, $p \leq 0.16$). Conversely to the WAVE IP data, we observed that VASP does associate with profilin (Fig. 22). As was seen with the WAVE assay, neither the Rac1 inhibitor (NSC23766) nor the Rho kinase inhibitor (Y27632) was sufficient to significantly decrease the complex formation of VASP with either profilin or Arp3 ($X^2 = 3.39$, $df = 5$, $p \leq 0.64$). Together these results indicate that while both WAVE and VASP associate with Arp3, differences exist between the complex components which drive nucleation and linear polymerization. Specifically, profilin is not associated with the complex containing WAVE and Arp3 (nucleation as side chains), but is present in the VASP and Arp3 complex (polymerization from the barbed end).

Figure 20: WAVE does not bind to profilin. The blots depict either cell lysates (bottom blot) or samples subjected to the immunoprecipitation protocol (top blot). Both blots were probed for profilin (~14 kDa).

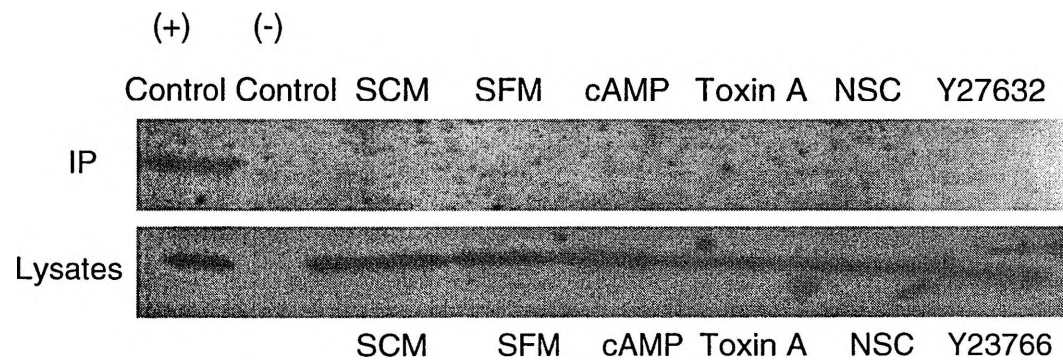


Figure 21: VASP binds to Arp3. The blots depict either cell lysates (A, bottom blot) or samples subjected to the immunoprecipitation protocol (A, top blot). Both blots were probed for Arp3 (~50 kDa). The graph represents average band intensities \pm SEM; n = 3 separate samples (B).

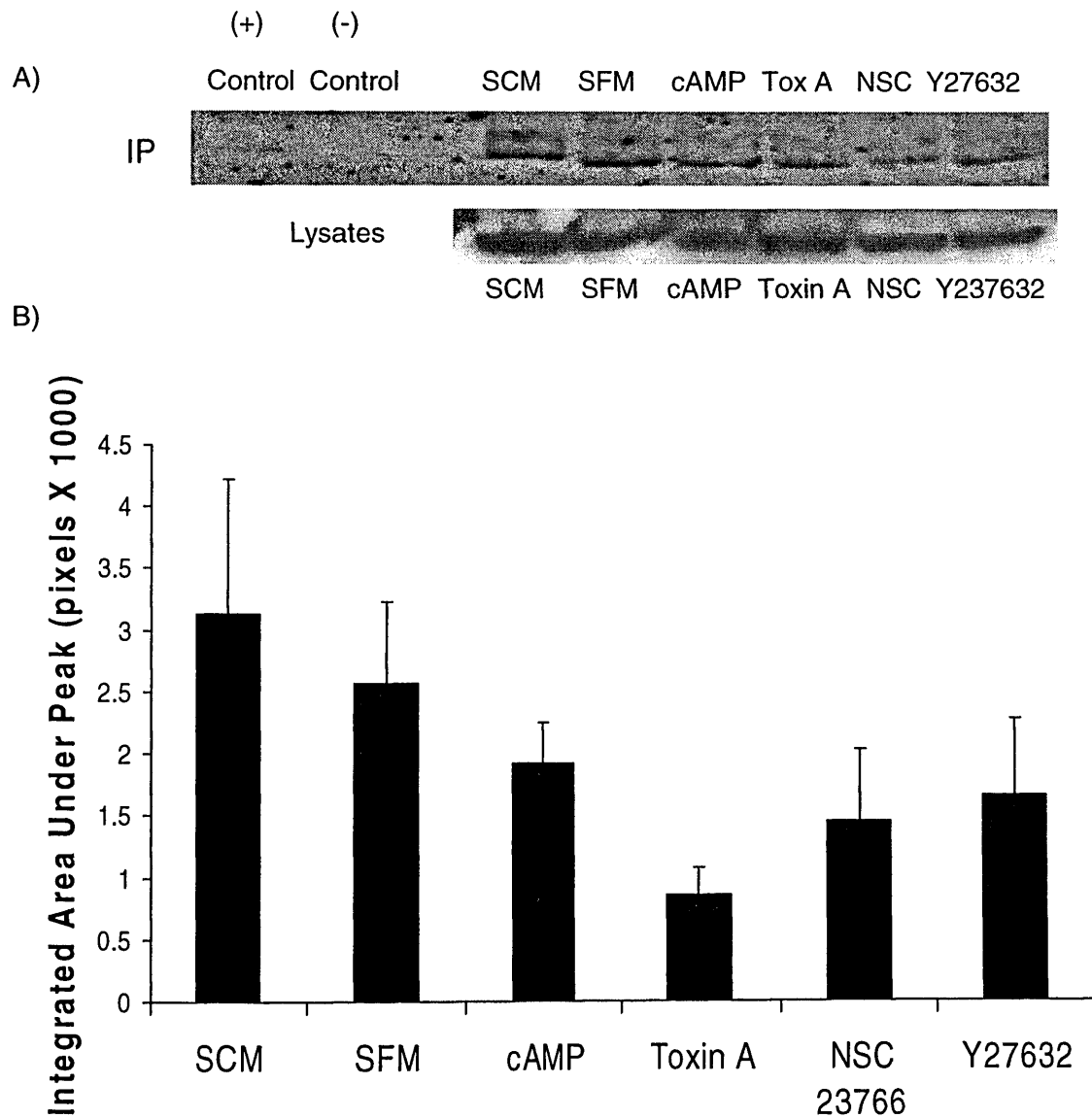
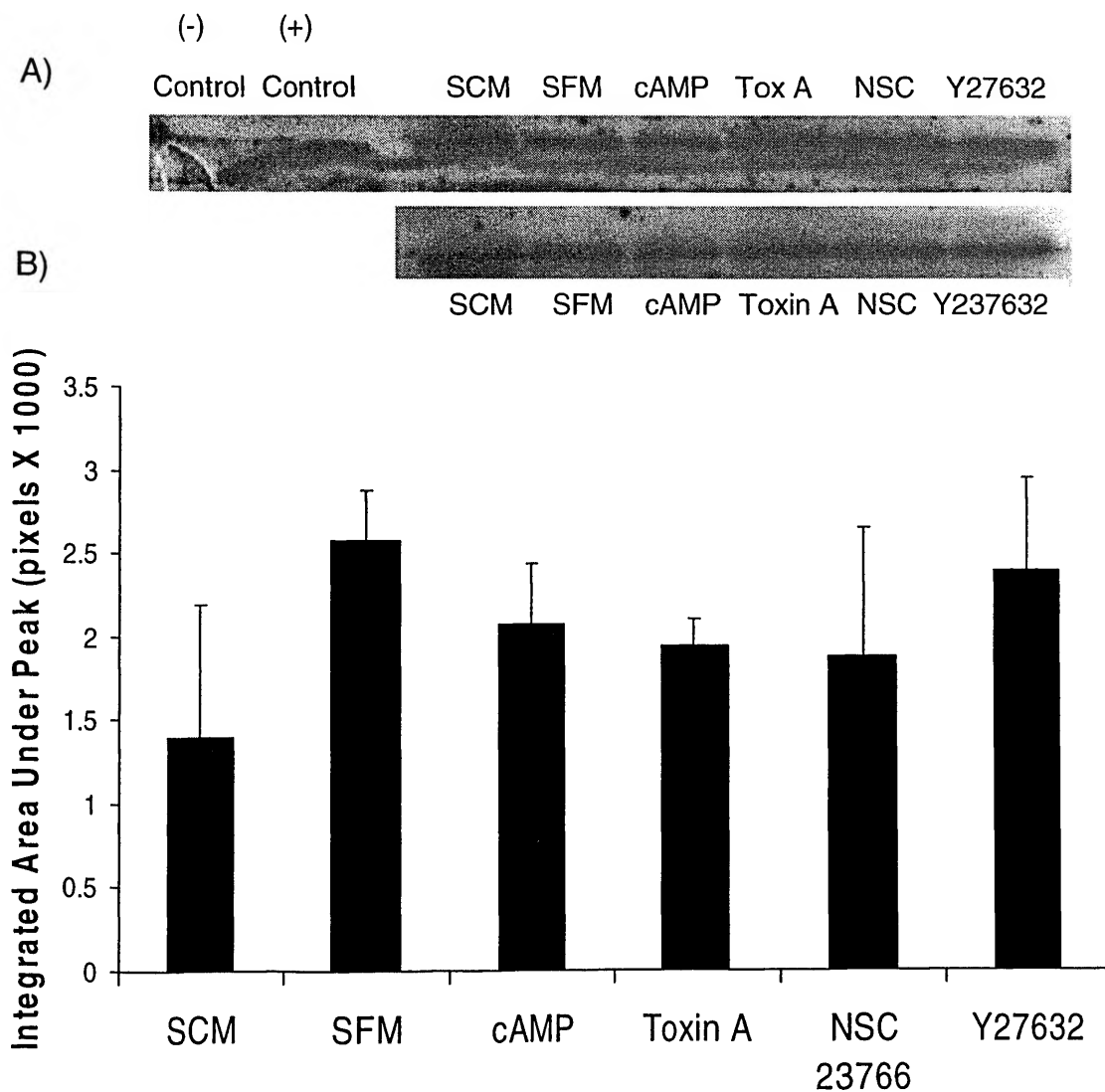


Figure 22: VASP binds to profilin. The blots depict either cell lysates (A, bottom blot) or samples subjected to the immunoprecipitation protocol (A, top blot). Both blots were probed for profilin (~14 kDa). The graph represents average band intensities \pm SEM; n = 3 separate samples (B).



CHAPTER IV

DISCUSSION

Functional recovery after spinal cord injury requires correct reinnervation of axons across the scar site. These mechanisms of axon growth and guidance are regulated, in part, by the Rho GTPases. Work in non-neuronal cells has shown that Rho GTPase activation not only regulates outgrowth, but does so by signaling to the actin cytoskeleton through the complex formation of actin binding proteins. However, this has not been established for neuronal cell types.

In this study we hypothesized that outgrowth promoting treatments would activate Rac1 in the growth cone while inhibitory treatments would increase RhoA activation in the growth cone. We also predicted that treatments which activate Rac1 would produce co-localization and complex formation of actin binding proteins within the lamellipodial region of the growth cone. Conversely, we thought inhibitory treatments would promote lower levels of actin binding complexes. We have tested the localization of RhoA and Rac1 activation through pull-down assays and ELISA-based absorbance assays. We examined the co-localization and complexing of WAVE, Arp3, VASP and profilin through immunocytochemistry and co-immunoprecipitation.

Activation of Rho GTPases by Outgrowth Promoters and Inhibitors

We assessed Rho GTPase activation in response to physiologically relevant outgrowth promoters and inhibitors. To promote outgrowth we used a cAMP analog (8-Br-cAMP) because cAMP production is increased by many chemo- and contact-attractants such as laminin (Bonner and O'Connor, 2001). Furthermore, in our model system (B35 neuroblastoma cells), both serum withdrawal and treatment with cAMP analogs increase outgrowth (Bhatt et al., 2002; Hynds et al., submitted). In general, results obtained in this study support previous work (Bonner and O'Connor, 2001). In particular, we found that serum withdrawal increased Rac1 activity and decreased RhoA activity. This is consistent with our hypothesis that outgrowth promoting treatments would increase Rac1 activation. Not expected, however, was the observation that Rac1 activation did not increase any more when 8-Br-cAMP was included along with SFM treatment. It is possible that the two treatments activate different signaling pathways that result in the same effect, or serum withdrawal itself could lead to an increase in cAMP. A third possibility is that regional differences in activation may occur, leading to compartmentalized effects of Rho GTPase activation.

Compartmentalization of Rho GTPase Activation

We hypothesized that treatments that increase outgrowth would lead to activation of Rac1 and inhibition of RhoA activity in the growth cones. Consistent with this, we found Rac1 to be preferentially activated in the growth cones by treatments that increase outgrowth. Interestingly, induction of RhoA activation was observed in both the somata and growth cones of B35 rat neuroblastoma cells. While the possibility exists that the differences in activation of Rac1 and RhoA could be attributed to varied distribution of the proteins, recent results in our lab show a uniform distribution of Rac1 and RhoA throughout B35 cells. More likely, in our opinion, is that the regional regulation of Rho GTPase activation may be accomplished by either differences in localization of GEFs, or sequestering by GDIs. PDZRhoGEF, a RhoA specific GEF, has been shown to regulate activation of RhoA and subsequently, its spatial distribution (Wong et al., 2007). A Rac specific GEF, Tiam1, also depends on localization to activate Rac1. Tiam1 must first bind to the Arp2/3 complex at sites of actin polymerization before it can modulate Rac1 activity (Ten Klooster et al., 2006). Differences in the localization of Rho GTPases regulators may contribute to the compartmentalization of Rho GTPase activation observed in our study.

Localization of Actin Binding Proteins Increases in the Growth Cone in Response to Outgrowth Promoting Treatments

Once we had established the activation ratios and compartmentalization of activation for Rac1 and RhoA in response to treatments which affect outgrowth, we chose to study the mechanisms by which the Rho GTPases regulate outgrowth. Actin dynamics within the lamellipodia are believed to drive growth cone advance (Meyer and Feldman, 2002; Matsuura et al., 2004). Given that we cannot observe Rho GTPase activation in specific regions of the growth cone (lamellipodia, filopodia, and central region) by biochemical methods, one approach is to look at the effects activation levels have on downstream effectors, such as actin binding proteins.

We hypothesized that treatments that increase Rac1 activity would increase complexing of actin binding proteins. Consistent with this, we found that treatments which promote outgrowth and activate Rac1 increased the number of immunopositive puncta for the actin binding proteins WAVE, VASP, Arp3, and profilin to all regions of the growth cone. Inhibition of all Rho GTPase signaling reduced the number of immunopositive puncta for these same proteins in the growth cone. These results are consistent with work done in both neuronal (Caprini et al., 2003; Da Silva et al., 2003) and non-neuronal cell types (Bear et al., 2000; Blanchoin et al., 2000). These studies show that actin binding proteins

are recruited to the leading edge of neurite extension or membrane protrusion during outgrowth.

Co-localization of Actin Binding Proteins Increases in the Growth Cone in Response to Outgrowth Promoting Treatments

Work in non-neuronal cells indicates that protrusion of structures at the leading edge of migrating cells is mediated by complexes of actin binding proteins formed subsequent to Rho GTPase activation. Actin binding proteins regulate actin depolymerization, polymerization of soluble (G) actin into filamentous (F) actin, nucleation (branching) of F-actin, and capping of F-actin at the barbed end (Schmidt et al., 1995; Meyer and Feldman, 2002). The molecular components of complexes of actin binding proteins have been studied extensively in non-neuronal cells. It has been shown that Arp2/3 forms a complex with WAVE and profilin as well as VASP and profilin to promote actin nucleation or actin polymerization (Mullins et al., 1998; Blanchoin et al., 2000; Caprini et al., 2003). In order to begin to study this in neuronal cells, we first determined if the proteins co-localized. Thus we looked at changes in the co-localization of four actin binding proteins: WAVE, VASP, Arp3, and profilin.

As we expected, co-localization of the actin binding proteins increased when treated with outgrowth promoting factors. This increase was generally not

seen when the cells were treated with either Toxin A (inhibits Rac1 and RhoA) or Y27632 (inhibits a downstream effector of RhoA) since treatments were carried out in SFM. What was not expected was the occasional increase in co-localization observed following treatment with the Rac1 inhibitor, NSC23766, when compared to SFM. It is possible that actin binding proteins are recruited to the growth cone and thus co-localize in a complex formation in response to Rac1 inhibition. Even though Rac1 was inhibited, Cdc42 was still active and presumably utilizing the actin binding proteins to promote actin polymerization within the filopodia. Also, active RhoA has been shown to signal through formins (Watanabe et al., 1999). Formins act to nucleate and bundle actin filaments. Possibly, these functions recruit actin binding proteins to the growth cone. We previously discussed that Rac1 activation promotes activation of RhoA (Sakumura et al., 2005). When Rac1 is inhibited (by NSC23766), RhoA activation levels may also be decreased. This leads to a decrease in actin filament retraction. This may partially explain the increase in co-localization of actin binding proteins observed following treatment which inhibits Rac1.

Molecular Components of Actin Binding Complexes are Different than Non-Neuronal Cells

After showing that an increase in co-localization of actin binding proteins corresponds with treatments that promote Rac1 activation and outgrowth, we wanted to determine if these proteins are bound to each other in a complex, at sites of actin polymerization, as had been previously shown in non-neuronal cells. We hypothesized that outgrowth promoting treatments would increase the amount of actin binding proteins complexed together. While we did not see significant differences in the amount of protein in each complex in response to treatments, we did find differences in complex components dependent on the function of that complex. Work in non-neuronal cells has shown that a complex of Arp2/3, WAVE, and profilin is responsible for the promotion of actin nucleation, while actin polymerization from barbed ends is promoted by a complex of VASP, Arp3 and profilin (Mullins et al., 1998).

Consistent with our hypothesis, we showed that WAVE and VASP both bind to Arp3, and VASP binds to profilin as expected. However, WAVE did not associate with profilin. This demonstrates that differences likely exist in the regulation of actin dynamics in neurons compared to non-neuronal cells. The difference in cytoarchitecture may result from such differential signaling. Another possibility is that the binding of profilin is transient and was not bound to WAVE

in our experimental conditions. Although in our experiment, we did not observe significant changes in complex formation in response to our treatment, there were some interesting trends. Outgrowth promoting treatments increased the binding of Arp3 and WAVE. This binding was decreased by the inhibitory treatments. Similarly, Toxin A also reduced the binding of Arp3 and VASP. Perhaps if we had performed the co-immunoprecipitation studies in growth cone fractions rather than whole cell lysates, the changes in complex formation in response to treatment would be more quantitative. Future studies will attempt to confirm the complex formations that we observed by precipitating with an Arp3 antibody and probing for profilin, WAVE and VASP.

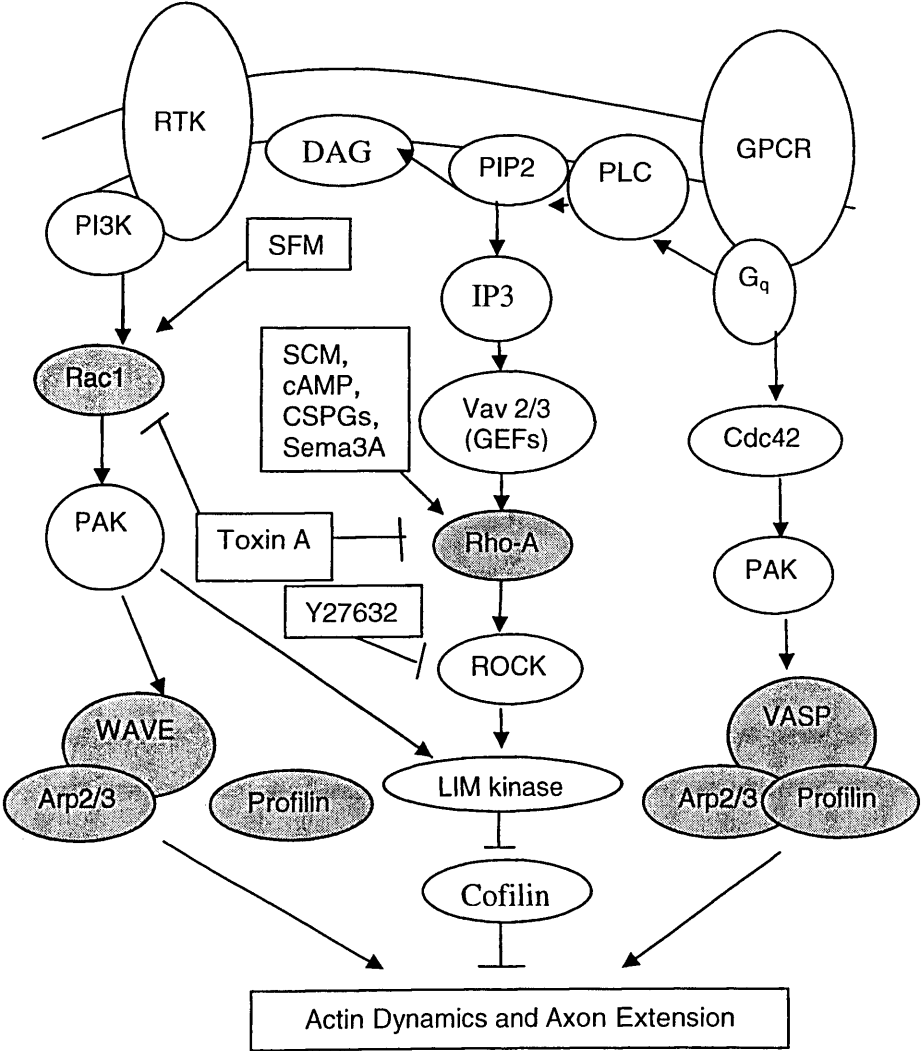
Rho GTPase Activation and Actin Binding Proteins

While the complex components did not significantly change across conditions, their location within the growth cone did. Treatments consistent with Rac1 activation recruited WAVE, profilin, Arp3 and VASP to the filopodial, lamellipodial, and central growth cone regions. In contrast, treatment consistent with inhibition of both Rac1 and RhoA reduced localization of WAVE, profilin, VASP, and Arp3 to all three regions of the growth cone. Thus, Rac1 activation may play a role in the regulation of neurite outgrowth through the recruitment of actin binding proteins to the growth cone in order to promote actin

polymerization. In particular, based on work in migratory cells, WAVE and Arp3 should complex and promote lamellipodial expansion (Abe et al., 2003). Our data support this as both are recruited to growth cones and complex in response to treatments known to increase Rac1 activation.

We propose the following model to explain our findings (Fig. 23). We found that SFM activated Rac1 while SCM, 8-Br-cAMP, CSPGs, and Sema3A activated RhoA. We also found that SFM increased the co-localization of actin binding proteins to the growth cone while Toxin A inhibited this recruitment. The factors tested in our study are shaded in gray. The treatments we utilized are presented in rectangular boxes. This model differs from the proposed model shown in the introduction in that profilin did not form a complex with WAVE and we did not see the expected inhibition of actin binding protein localization in response to treatment with the Rac1 inhibitor, NSC23766.

Figure 23: Proposed model for Rho GTPase activation and their associated effects on actin binding proteins. Shaded components indicate aspects of the proposed model which we tested, and treatments with their reported or proposed effects are indicated in rectangles. In this model, profilin is not in a complex with WAVE and NSC23766 treatment does not recruit actin binding proteins.



Summary

In conclusion, we have shown that treatments that increase outgrowth in B35 cells are associated with an increase in Rac1 and RhoA activation in growth cones, but a decrease in RhoA activation in cell bodies. Furthermore, increases in Rho GTPase activity in growth cones correlated with increased growth cone localization of actin binding proteins that promote complexes of actin nucleation and polymerization. Conversely, treatments that decrease outgrowth decreased Rac1 activity in growth cones but increased RhoA activity in somata. When Rho GTPase activity is inhibited, localization of actin binding proteins to growth cones is decreased. These data suggest that Rho GTPase activity leads to the recruitment of actin binding proteins to growth cones. When complexed, these actin binding proteins promote growth cone extension. However, co-immunoprecipitation data indicate that members of complexes of actin binding proteins may be different in neuronal and non-neuronal cells. Elucidation of the regulatory pathways governing Rho GTPase activation and actin dynamics in neuronal cells may provide insight into mechanisms of axon regeneration and might be used to develop therapeutic strategies to treat central nervous system damage like spinal cord injury.

REFERENCES

- Abe T, Kato M, Miki H, Takenawa T, Endo T (2003) Small GTPase Tc10 and its homologue RhoT induce N-WASP-mediated long process formation and neurite outgrowth. *J Cell Sci* 116:155-168.
- Alberts AS (2001) Identification of a carboxyl-terminal diaphanous-related formin homology protein autoregulatory domain. *J Biol Chem* 276:2824-2830.
- Altun-Gultekin ZF, Chandriani S, Bougeret C, Ishizaki T, Narumiya S, de Graaf P, Van Bergen en Henegouwen P, Hanafusa H, Wagner JA, Birge RB (1998) Activation of Rho-dependent cell spreading and focal adhesion biogenesis by the v-Crk adaptor protein. *Mol Cell Biol* 18:3044-3058.
- Arber S, Barbayannis FA, Hanser H, Schneider C, Stanyon CA, Bernard O, Caroni P (1998) Regulation of actin dynamics through phosphorylation of cofilin by LIM-kinase. *Nature* 393:805-809.
- Bear JE, Loureiro JJ, Libova I, Fassler R, Wehland J, Gertler FB (2000) Negative regulation of fibroblast motility by Ena/VASP proteins. *Cell* 101:717-728.
- Beavo JA, Reifsnyder DH (1990) Primary sequence of cyclic nucleotide phosphodiesterase isozymes and the design of selective inhibitors. *Trends Pharmacol Sci* 11:150-155.

- Benard V, Bohl BP, Bokoch GM (1999) Characterization of Rac and Cdc42 activation in chemoattractant-stimulated human neutrophils using a novel assay for active GTPases. *J Biol Chem* 274:13198-13204.
- Bishop AL, Hall A (2000) Rho GTPases and their effector proteins. *Biochem J* 348 Pt 2:241-255.
- Bito H, Furuyashiki T, Ishihara H, Shibasaki Y, Ohashi K, Mizuno K, Maekawa M, Ishizaki T, Narumiya S (2000) A critical role for a Rho-associated kinase, p160^{ROCK}, in determining axon outgrowth in mammalian CNS neurons. *Neuron* 26:431-441.
- Blanchoin L, Pollard TD, Mullins RD (2000) Interactions of ADF/cofilin, Arp2/3 complex, capping protein and profilin in remodeling of branched actin filament networks. *Curr Biol* 10:1273-1282.
- Bonner J, O'Connor TP (2001) The permissive cue laminin is essential for growth cone turning in vivo. *J Neurosci* 21:9782-9791.
- Buchsbaum RJ, Connolly BA, Feig LA (2002) Interaction of Rac exchange factors Tiam1 and Ras-GRF1 with a scaffold for the p38 mitogen-activated protein kinase cascade. *Mol Cell Biol* 22:4073-4085.
- Caprini M, Gomis A, Cabedo H, Planells-Cases R, Belmonte C, Viana F, Ferrer-Montiel A (2003) GAP43 stimulates inositol trisphosphate-mediated calcium release in response to hypotonicity. *Embo J* 22:3004-3014.

- Choi EJ, Xia Z, Villacres EC, Storm DR (1993) The regulatory diversity of the mammalian adenylyl cyclases. *Curr Opin Cell Biol* 5:269-273.
- Costigan M, Mannion RJ, Kendall G, Lewis SE, Campagna JA, Coggeshall RE, Meridith-Middleton J, Tate S, Woolf CJ (1998) Heat shock protein 27: developmental regulation and expression after peripheral nerve injury. *J Neurosci* 18:5891-5900.
- Da Silva JS, Medina M, Zuliani C, Di Nardo A, Witke W, Dotti CG (2003) RhoA/ROCK regulation of neuritogenesis via profilin IIa-mediated control of actin stability. *J Cell Biol* 162:1267-1279.
- del Pozo MA, Price LS, Alderson NB, Ren XD, Schwartz MA (2000) Adhesion to the extracellular matrix regulates the coupling of the small GTPase Rac to its effector PAK. *Embo J* 19:2008-2014.
- Edwards DC, Sanders LC, Bokoch GM, Gill GN (1999) Activation of LIM-kinase by PAK1 couples Rac/Cdc42 GTPase signalling to actin cytoskeletal dynamics. *Nat Cell Biol* 1:253-259.
- Etienne-Manneville S, Hall A (2002) Rho GTPases in cell biology. *Nature* 420:629-635.
- Gallo G, Letourneau PC (2004) Regulation of growth cone actin filaments by guidance cues. *J Neurobiol* 58:92-102.

- Garcia Arguinzonis MI, Galler AB, Walter U, Reinhard M, Simm A (2002) Increased spreading, Rac/p21-activated kinase (PAK) activity, and compromised cell motility in cells deficient in vasodilator-stimulated phosphoprotein (VASP). *J Biol Chem* 277:45604-45610.
- Govek EE, Newey SE, Van Aelst L (2005) The role of the Rho GTPases in neuronal development. *Genes Dev* 19:1-49.
- Gutkind JS (1998) The pathways connecting G protein-coupled receptors to the nucleus through divergent mitogen-activated protein kinase cascades. *J Biol Chem* 273:1839-1842.
- Hall C, Brown M, Jacobs T, Ferrari G, Cann N, Teo M, Monfries C, Lim L (2001) Collapsin response mediator protein switches RhoA and Rac1 morphology in N1E-115 neuroblastoma cells and is regulated by Rho kinase. *J Biol Chem* 276:43482-43486.
- Harris ES, Rouiller I, Hanein D, Higgs HN (2006) Mechanistic differences in actin bundling activity of two mammalian formins, FRL1 and mDia2. *J Biol Chem* 281:14383-14392.
- Hell JW, Westenbroek RE, Elliott EM, Catterall WA (1994) Differential phosphorylation, localization, and function of distinct alpha 1 subunits of neuronal calcium channels. Two size forms for class B, C, and D alpha 1 subunits with different COOH-termini. *Ann N Y Acad Sci* 747:282-293.

- Jaffe AB, Aspenstrom P, Hall A (2004) Human CNK1 acts as a scaffold protein, linking Rho and Ras signal transduction pathways. *Mol Cell Biol* 24:1736-1746.
- Jain A, Brady-Kalnay SM, Bellamkonda RV (2004) Modulation of Rho GTPase activity alleviates chondroitin sulfate proteoglycan-dependent inhibition of neurite extension. *J Neurosci Res* 77:299-307.
- Jin M, Guan CB, Jiang YA, Chen G, Zhao CT, Cui K, Song YQ, Wu CP, Poo MM, Yuan XB (2005) Ca^{2+} -dependent regulation of rho GTPases triggers turning of nerve growth cones. *J Neurosci* 25:2338-2347.
- Knaus UG, Bokoch GM (1998) The p21Rac/Cdc42-activated kinases (PAKs). *Int J Biochem Cell Biol* 30:857-862.
- Kozma R, Sarner S, Ahmed S, Lim L (1997) Rho family GTPases and neuronal growth cone remodelling: relationship between increased complexity induced by Cdc42Hs, Rac1, and acetylcholine and collapse induced by RhoA and lysophosphatidic acid. *Mol Cell Biol* 17:1201-1211.
- Kranenburg O, Poland M, van Horck FP, Drechsel D, Hall A, Moolenaar WH (1999) Activation of RhoA by lysophosphatidic acid and $G_{\alpha 12/13}$ subunits in neuronal cells: induction of neurite retraction. *Mol Biol Cell* 10:1851-1857.

- Kuhn TB, Brown MD, Wilcox CL, Raper JA, Bamberg JR (1999) Myelin and Collapsin-1 Induce Motor Neuron Growth Cone Collapse through Different Pathways: Inhibition of Collapse by Opposing Mutants of Rac1. *J Neurosci* 19:1965-1975.
- Li W, Hu P, Skolnik EY, Ullrich A, Schlessinger J (1992) The SH2 and SH3 domain-containing Nck protein is oncogenic and a common target for phosphorylation by different surface receptors. *Mol Cell Biol* 12:5824-5833.
- Liu BP, Chrzanowska-Wodnicka M, Burridge K (1998) Microtubule depolymerization induces stress fibers, focal adhesions, and DNA synthesis via the GTP-binding protein Rho. *Cell Adhes Commun* 5:249-255.
- Loudon RP, Silver LD, Yee HF, Jr., Gallo G (2006) RhoA-kinase and myosin II are required for the maintenance of growth cone polarity and guidance by nerve growth factor. *J Neurobiol*.
- Mackay DJ, Nobes CD, Hall A (1995) The Rho's progress: a potential role during neuritogenesis for the Rho family of GTPases. *Trends Neurosci* 18:496-501.

Matsuura R, Tanaka H, Go MJ (2004) Distinct functions of Rac1 and Cdc42 during axon guidance and growth cone morphogenesis in *Drosophila*. *Eur J Neurosci* 19:21-31.

Meberg PJ, Ono S, Minamide LS, Takahashi M, Bamburg JR (1998) Actin depolymerizing factor and cofilin phosphorylation dynamics: response to signals that regulate neurite extension. *Cell Motil Cytoskeleton* 39:172-190.

Meyer G, Feldman EL (2002) Signaling mechanisms that regulate actin-based motility processes in the nervous system. *J Neurochem* 83:490-503.

Meyerson G, Pfenninger KH, Pahlman S (1992) A complex consisting of pp60c-src/pp60c-srcN and a 38 kDa protein is highly enriched in growth cones from differentiated SH-SY5Y neuroblastoma cells. *J Cell Sci* 103 (Pt 1):233-243.

Moolenaar WH, Kranenburg O, Postma FR, Zondag GC (1997) Lysophosphatidic acid: G-protein signalling and cellular responses. *Curr Opin Cell Biol* 9:168-173.

Moseley JB, Maiti S, Goode BL (2006) Formin proteins: purification and measurement of effects on actin assembly. *Methods Enzymol* 406:215-234.

- Mullins RD, Heuser JA, Pollard TD (1998) The interaction of Arp2/3 complex with actin: nucleation, high affinity pointed end capping, and formation of branching networks of filaments. *Proc Natl Acad Sci U S A* 95:6181-6186.
- Nakamura T, Aoki K, Matsuda M (2005) FRET imaging in nerve growth cones reveals a high level of RhoA activity within the peripheral domain. *Brain Res Mol Brain Res* 139:277-287.
- Newey SE, Velamoor V, Govak EE, Van Aelst L (2005) Rho GTPases, dendritic structure, and mental retardation. *J Neurobiol* 64:58-74.
- Niederost B, Oertle T, Fritsche J, McKinney RA, Bandtlow CE (2002) Nogo-A and myelin-associated glycoprotein mediate neurite growth inhibition by antagonistic regulation of RhoA and Rac1. *J Neurosci* 22:10368-10376.
- Nishimura R, Li W, Kashishian A, Mondino A, Zhou M, Cooper J, Schlessinger J (1993) Two signaling molecules share a phosphotyrosine-containing binding site in the platelet-derived growth factor receptor. *Mol Cell Biol* 13:6889-6896.
- Nishiyama M, Hoshino A, Tsai L, Henley JR, Goshima Y, Tessier-Lavigne M, Poo M-m, Hong K (2003) Cyclic AMP/GMP-dependent modulation of Ca²⁺ channels sets the polarity of nerve growth-cone turning. *Nature* 423:990-995.

- Nusser N, Gosmanova E, Makarova N, Fujiwara Y, Yang L, Guo F, Luo Y, Zheng Y, Tigyi G (2005) Serine phosphorylation differentially affects RhoA binding to effectors: Implications to NGF-induced neurite outgrowth. *Cell Signal*.
- Otey CA, Boukhelifa M, Maness P (2003) B35 neuroblastoma cells: an easily transfected, cultured cell model of central nervous system neurons. *Methods Cell Biol* 71:287-304.
- Pruyne D, Evangelista M, Yang C, Bi E, Zigmond S, Bretscher A, Boone C (2002) Role of formins in actin assembly: nucleation and barbed-end association. *Science* 297:612-615.
- Raper JA (2000) Semaphorins and their receptors in vertebrates and invertebrates. *Curr Opin Neurobiol* 10:88-94.
- Rashid T, Banerjee M, Nikolic M (2001) Phosphorylation of PAK1 by the p35/Cdk5 kinase affects neuronal morphology. *J Biol Chem* 276:49043-49052.
- Ridley AJ, Hall A (1992) The small GTP-binding protein rho regulates the assembly of focal adhesions and actin stress fibers in response to growth factors. *Cell* 70:389-399.
- Ridley AJ, Allen WE, Peppelenbosch M, Jones GE (1999) Rho family proteins and cell migration. *Biochem Soc Symp* 65:111-123.

- Ridley AJ, Paterson HF, Johnston CL, Diekmann D, Hall A (1992) The small GTP-binding protein Rac regulates growth factor-induced membrane ruffling. *Cell* 70:401-410.
- Ridley AJ, Schwartz MA, Burridge K, Firtel RA, Ginsberg MH, Borisy G, Parsons JT, Horwitz AR (2003) Cell migration: integrating signals from front to back. *Science* 302:1704-1709.
- Rosdahl JA, Ensslen SE, Niedenthal JA, Brady-Kalnay SM (2003) PTP mu-dependent growth cone rearrangement is regulated by Cdc42. *J Neurobiol* 56:199-208.
- Sagot I, Rodal AA, Moseley J, Goode BL, Pellman D (2002) An actin nucleation mechanism mediated by Bni1 and profilin. *Nat Cell Biol* 4:626-631.
- Sakumura Y, Tsukada Y, Yamamoto N, Ishii S (2005) A molecular model for axon guidance based on cross talk between rho GTPases. *Biophys J* 89:812-822.
- Schaefer AW, Kabir N, Forscher P (2002) Filopodia and actin arcs guide the assembly and transport of two populations of microtubules with unique dynamic parameters in neuronal growth cones. *J Cell Biol* 158:139-152.
- Schmidt CE, Dai J, Lauffenburger DA, Sheetz MP, Horwitz AF (1995) Integrin-cytoskeletal interactions in neuronal growth cones. *J Neurosci* 15:3400-3407.

- Singleton PA, Bourguignon LY (2002) CD44v10 interaction with Rho-kinase (ROK) activates inositol 1,4,5-triphosphate (IP3) receptor-mediated Ca^{2+} signaling during hyaluronan (HA)-induced endothelial cell migration. *Cell Motil Cytoskeleton* 53:293-316.
- Spencer T, Domeniconi M, Cao Z, Filbin MT (2003) New roles for old proteins in adult CNS axonal regeneration. *Curr Opin Neurobiol* 13:133-139.
- Stettler O, Bush MS, Kasper M, Schlosshauer B, Gordon-Weeks PR (1999) Monoclonal antibody 2G13, a new axonal growth cone marker. *J Neurocytol* 28:1035-1044.
- Stossel TP (1993) On the crawling of animal cells. *Science* 260:1086-1094.
- Suter DM, Schaefer AW, Forscher P (2004) Microtubule dynamics are necessary for SRC family kinase-dependent growth cone steering. *Curr Biol* 14:1194-1199.
- Swiercz JM, Kuner R, Offermanns S (2004) Plexin-B1/RhoGEF-mediated RhoA activation involves the receptor tyrosine kinase ErbB-2. *J Cell Biol* 165:869-880.
- Swiercz JM, Kuner R, Behrens J, Offermanns S (2002) Plexin-B1 directly interacts with PDZ-RhoGEF/LARG to regulate RhoA and growth cone morphology. *Neuron* 35:51-63.

- Symons M (2000) Adhesion signaling: PAK meets Rac on solid ground. *Curr Biol* 10:R535-537.
- Tamagnone L, Comoglio PM (2000) Signalling by semaphorin receptors: cell guidance and beyond. *Trends Cell Biol* 10:377-383.
- Tamagnone L, Artigiani S, Chen H, He Z, Ming GI, Song H, Chedotal A, Winberg ML, Goodman CS, Poo M, Tessier-Lavigne M, Comoglio PM (1999) Plexins are a large family of receptors for transmembrane, secreted, and GPI-anchored semaphorins in vertebrates. *Cell* 99:71-80.
- Ten Klooster JP, Evers EE, Janssen L, Machesky LM, Michiels F, Hordijk P, Collard JG (2006) Interaction between Tiam1 and the Arp2/3 complex links activation of Rac to actin polymerization. *Biochem J* 397:39-45.
- Tigyi G, Fischer DJ, Sebok A, Yang C, Dyer DL, Miledi R (1996) Lysophosphatidic acid-induced neurite retraction in PC12 cells: control by phosphoinositide-Ca²⁺ signaling and Rho. *J Neurochem* 66:537-548.
- Vastrik I, Eickholt BJ, Walsh FS, Ridley A, Doherty P (1999) Sema3A-induced growth-cone collapse is mediated by Rac1 amino acids 17-32. *Curr Biol* 9:991-998.
- Vikis HG, Li W, Guan KL (2002) The plexin-B1/Rac interaction inhibits PAK activation and enhances Sema4D ligand binding. *Genes Dev* 16:836-845.

- Wahl S, Barth H, Ciossek T, Aktories K, Mueller BK (2000) Ephrin-A5 induces collapse of growth cones by activating Rho and Rho kinase. *J Cell Biol* 149:263-270.
- Watanabe N, Kato T, Fujita A, Ishizaki T, Narumiya S (1999) Cooperation between mDia1 and ROCK in Rho-induced actin reorganization. *Nat Cell Biol* 1:136-143.
- Witke W, Sutherland JD, Sharpe A, Arai M, Kwiatkowski DJ (2001) Profilin I is essential for cell survival and cell division in early mouse development. *Proc Natl Acad Sci U S A* 98:3832-3836.
- Wong K, Van Keymeulen A, Bourne HR (2007) PDZRhoGEF and myosin II localize RhoA activity to the back of polarizing neutrophil-like cells. *J Cell Biol* 179:1141-1148.

APPENDIX
LIST OF ABBREVIATIONS

ALS.....	amyotrophic lateral sclerosis
ANOVA.....	analysis of variance
8-Br-cAMP.....	8-bromoadenosine-5',3'-cyclic monophosphate
cAMP.....	5',3'-cyclic monophosphate
CSPGs.....	chondroitin sulfate proteoglycans
DAG.....	diacylglycerol
DAPI.....	4',6-Diamidino-2-Phenylindole
DIC.....	differential interference contrast
DMEM.....	Dulbecco's modified Eagle medium
ECM.....	extracellular matrix
EGF.....	epidermal growth factor
ELISA.....	enzyme-linked immunoabsorbance
F actin.....	filamentous actin
FBS.....	fetal bovine system
FRET.....	fluorescence resonance energy transfer
G actin.....	globular actin
GAP.....	GTPase activating protein

GDI.....guanine nucleotide dissociation inhibitor

GEF..... guanine nucleotide exchange factor

GPCR.....G-protein coupled receptor

GTPase..... guanine nucleotide triphosphatase

HRP.....horseradish peroxidase

IgG.....immunoglobulin

IP.....immunoprecipitation

IP3.....inositol triphosphate

LPA..... lysophosphatidic acid

MAG.....myelin-associated glycoprotein

MAPK..... mitogen-activated protein kinase

NGF.....nerve growth factor

PAK.....p21-activated kinase

PBS..... phosphate buffered saline

PDGF.....platelet derived growth factor

PI3 Kinase.....phosphatidylinositol 3-kinase

PIP₂..... phosphatidylinositol 4,5-bisphosphate

PIP₃.....phosphatidylinositol 3,4,5-trisphosphate

PKC.....protein kinase C

RA.....retinoic acid

ROCK..... Rho-associated, coiled-coil-forming protein kinase
RTK.....receptor tyrosine kinase
Sema3A.....semaphorin 3A
SFM.....serum free media
SCM.....serum containing media
TBS.....tris-buffered saline
TBST.....tris-buffered saline with Tween
WASP.....Wiskott-Aldrich syndrome protein